Stochastic modelling of reaction-diffusion processes: algorithms for bimolecular reactions

Radek Erban and S. Jonathan Chapman

University of Oxford, Mathematical Institute, 24-29 St. Giles', Oxford, OX1 3LB, United Kingdom

E-mail: `erban@maths.ox.ac.uk`; `chapman@maths.ox.ac.uk`

Abstract. Several stochastic simulation algorithms (SSAs) have been recently proposed for modelling reaction-diffusion processes in cellular and molecular biology. In this paper, two commonly used SSAs are studied. The first SSA is an on-lattice model described by the reaction-diffusion master equation. The second SSA is an off-lattice model based on the simulation of Brownian motion of individual molecules and their reactive collisions. In both cases, it is shown that the commonly used implementation of bimolecular reactions (i.e. the reactions of the form $A+B \to C$, or $A+A \to C$) might lead to incorrect results. Improvements of both SSAs are suggested which overcome the difficulties highlighted. In particular, a formula is presented for the smallest possible compartment size (lattice spacing) which can be correctly implemented in the first model. This implementation uses a new formula for the rate of bimolecular reactions per compartment (lattice site).

Keywords: stochastic simulation, reaction-diffusion problems, bimolecular reactions.

1. Introduction

Many cellular and subcellular biological processes can be described in terms of diffusing and chemically reacting species (e.g. enzymes) [1, 13]. A traditional approach to the mathematical modelling of such reaction-diffusion processes is to describe each (bio)chemical species by its (spatially-dependent) concentration. The time evolution of concentrations is then modelled by a system of partial differential equations (PDEs) [29]. Many mathematical and computational methods have been developed over the last century for solving and analyzing PDEs [35, 40], which makes PDE-based modelling attractive. However, it has serious limitations when applied to biological systems. There may be relatively few numbers of some chemical species; for example, often only one or two mRNA molecules of a particular gene are present in the cell [1]. In such cases we cannot even properly define spatially-dependent concentration profiles* and PDE-

---

* The macroscopic concentration of molecules at a given point in the space is defined as the number of molecules in a neighbourhood of this point divided by the volume of the neighbourhood. In particular, the neighbourhood must be chosen large enough to contain a lot of molecules. This is clearly not possible if there are only few molecules present in the system.

based models cannot be used. The appropriate quantities to describe the system are not concentrations, but numbers and positions of molecules of the chemical species involved.

In recent years, several stochastic simulation algorithms (SSAs) have been proposed to model the time evolution of molecular numbers [24, 3, 13]. They provide a more detailed and precise picture than deterministic PDE-based models. They typically give the same results for simple systems involving zero-order and first-order chemical reactions (for example, linear degradation or conversion). However, the situation is more delicate whenever some chemical species are subject to bimolecular (second-order) reactions, or the system under study includes reactive boundaries (for example, a cellular membrane with receptors). Reactive boundaries were studied in our previous paper [13], where we systematically investigated four different SSAs for reaction-diffusion processes which had been proposed in the literature. We showed that one would obtain incorrect results if the computer implementation of reactive boundaries is not handled with care. In particular, different results can be obtained by different SSAs when using what seems to be, on the face of it, the same boundary condition. To fix this problem, we derived formulae giving the correct relation between experimentally measurable characteristics and parameters of the computer implementation of boundary conditions for all four SSAs [13]. A generalization of one of these formulae to anisotropic diffusion tensors was recently given in [32].

In this paper, we focus on modelling bimolecular reactions, i.e. chemical reactions of the form $A+B \rightarrow C$ or $A+A \rightarrow C$. We investigate two commonly used reaction-diffusion SSAs which have been previously implemented in reaction-diffusion software packages MesoRD [24] and Smoldyn [3]. The first reaction-diffusion SSA is based on dividing the computational domain into artificially well-mixed compartments and postulating that only molecules which are within the same compartment can react. Diffusion is then modelled as jumps between the neighbouring compartments. This approach can be mathematically described by the reaction-diffusion master equation [27, 12, 16] and was recently implemented in the mesoscopic reaction-diffusion simulator MesoRD [24]. In order to use this method, we have to choose an appropriate compartment size. On one hand, the compartment size must be chosen small enough so that the spatial variation in the concentration profiles can be captured with a desired resolution. The situation is analogous to solving PDEs numerically by a finite difference method. In order to solve PDEs with the desired accuracy, we need to choose a sufficiently fine mesh for discretization. On the other hand, we will see in Section 3.1 that the compartment size cannot be chosen arbitrarily small. The analogy with PDEs fails here. Unlike in the case of PDEs (for which we get a more accurate solution by using a finer discretization), there is a limit on the compartment size from below. In Section 3.1, we will show that the error of the computation increases as the compartment size decreases. In Section 4.1, we present the formula for the smallest compartment size (which can be simulated by this approach) and propose an improved SSA which minimizes the simulation error, by modifying the reaction rate per compartment.

The second SSA studied in this paper is based on Brownian motion of individual

molecules. In its classical formulation [33], it is postulated that two molecules (which are subject to a bimolecular reaction) react whenever they are within a specified distance (reaction radius) from each other. One disadvantage of this approach is that the reaction radius is, for typical values of the bimolecular rate constant and diffusion coefficient, unrealistically small compared to the size of individual molecules. In Section 4.2, we propose an improved SSA to overcome this difficulty. It is based on the assumption that two molecules react with the rate λ whenever they are within the distance $\overline{\varrho}$. The formula relating λ, $\overline{\varrho}$ and the simulation time step with the experimentally measurable reaction rate constant is derived. This formula is used for developing a more realistic SSA for reaction-diffusion processes. In particular, we generalize the approach recently implemented in the software package Smoldyn [3].

The paper is organized as follows. In Section 2, we present illustrative examples which will be used to demonstrate the results of the paper. In Section 3, we present both reaction-diffusion SSAs and summarize their major disadvantages. In Section 4, we present modified algorithms which are able to overcome the problems highlighted in Section 3. To make this paper accessible to non-mathematicians, Section 4 only contains the description of improved algorithms and formulae, together with the results of illustrative computations. The mathematical derivation of the formulae presented and the justification of the modified algorithms are given in Appendices. We finish with a discussion and conclusions in Section 5.

2. Bimolecular reactions - two model problems

A bimolecular reaction is a chemical reaction involving two reacting molecules. Examples include

$$A + B \xrightarrow{k} C + D, \qquad A + A \xrightarrow{k} C, \qquad \text{or} \qquad A + B \xrightarrow{k} B,$$

where the capital letters A, B, C stand for chemical species and k is the reaction rate constant, expressed in units of volume over time. From the modelling point of view, it is useful to divide bimolecular reactions into two classes, heteroreactions and homoreactions. The term *heteroreaction* will be used for the bimolecular reaction between molecules of two different chemical species (for example, heterodimerization $A + B \rightarrow C$ or catalytic degradation $A + B \rightarrow B$). The bimolecular reaction between two molecules of the same chemical species (for example, homodimerization $A + A \rightarrow C$) will be called the *homoreaction* in what follows. In this section, we introduce two simple chemical systems which will be used to illustrate the results in the paper. The first model will include a heteroreaction (catalytic degradation) and the second model a homoreaction (homodimerization). More complicated examples are discussed later in Section 5.

2.1. A heteroreaction example

Let us consider chemical species A and B in a container of volume ν which are subject to the following two chemical reactions

$$A + B \xrightarrow{k_1} B, \qquad \emptyset \xrightarrow{k_2} A. \qquad (1)$$

The first reaction is the degradation of A catalyzed by B. We couple it with the second reaction which represents the production of molecules of A with the rate* $k_2\nu$. Since the number of B molecules is preserved in the chemical reactions (1), the dynamics of the model (1) is simple: some molecules of A are produced by the second reaction and some are destroyed by the first reaction. Thus, after an initial transient behaviour, the number of A molecules fluctuates around its equilibrium value.

Let us consider first the case when the chemical system (1) is well-stirred. Then the probability of an ocurrence of the bimolecular reaction is proportial to the number of available pairs of reactants [21]. Let us define the propensity functions of chemical reactions (1) by

$$\alpha_1(t) = A(t)B(t)k_1/\nu, \qquad \alpha_2(t) = k_2\nu \qquad (2)$$

where $A(t)$ is the number of molecules of A at time t, $B(t)$ is the number of molecules of B at time t, and ν is the system volume. Then the probability that the i-th reaction occurs in the infinitesimally small time interval $[t, t + \mathrm{d}t)$ is equal to $\alpha_i(t)\,\mathrm{d}t$, $i = 1, 2$. Note that any heteroreaction $A + B \to \cdots$ has a propensity function equal to $\alpha_1(t)$, while the propensity function of homoreactions differs; this is the reason why we discuss them separately.

The chance of occurrence of each reaction is given by the corresponding propensity function (2). If the first chemical reaction occurs, then one molecule of A is removed from the system; if the second chemical reaction takes places, then one molecule of A is added to the system. Given the values of the rate constants and the initial numbers of molecules of A and B, the stochastic model of (1) is uniquely specified and can be simulated by the Gillespie SSA [21, 22]. In Figure 1(a), we plot $A(t)$, computed by the Gillespie SSA, as the solid line, using parameter values $k_1/\nu = 0.2\,\mathrm{sec}^{-1}$, $k_2\nu = 1\,\mathrm{sec}^{-1}$, $A(0) = 5$ and $B(0) = 1$. As expected the number of molecules of A fluctuates around the average value which is 5 for our parameters. The nature of these fluctuations can be summarized in terms of the *stationary distribution*. To compute it, we record the values of $A(t)$ at equal time intervals and create a histogram of the recorded values. Dividing the histogram by the total number of recordings, we obtain distribution $\phi(n)$ which is plotted in Figure 1(b) as the grey histogram. Thus, $\phi(n)$ is the probability that there are n molecules of A in the system, provided that the system is observed for a sufficiently long time. Note that since the Gillespie SSA makes use of random numbers to compute the time evolution of the system, the computed $A(t)$ depends on a particular realization of the algorithm. Repeating the computation (with a different

---

* Let us note that k_2 (the rate constant of the zero-order reaction) has physical dimension of units per volume per time. Consequently, $k_2\nu$ is expressed in units per time.
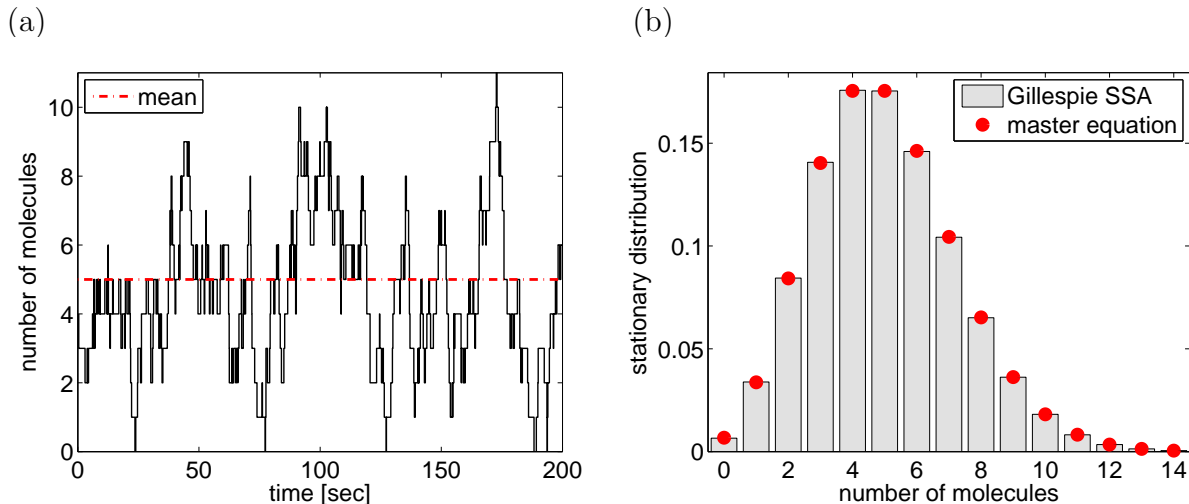
(a)

(b)

Figure 1. *Stochastic simulation of the system of chemical reactions (1) for $k_1/\nu = 0.2\,\mathrm{sec}^{-1}$, $k_2\nu = 1\,\mathrm{sec}^{-1}$ and one molecule of B in the system. (a) $A(t)$ given by one realization of the Gillespie SSA (solid line) for the initial value $A(0) = 5$. The average value of A is plotted as the dashed line. (b) Stationary distribution $\phi(n)$ obtained by long time simulation of the Gillespie SSA (grey histogram) and by formula (3) (circles).*

set of random numbers), we will obtain a different time evolution than the one plotted in Figure 1(a). However, the stationary distribution $\phi(n)$ is uniquely determined by the values of the rate constants k_1, k_2 and the number of molecules of B in the container. It can be shown (see Appendix A) that $\phi(n)$ is the Poisson distribution

$$\phi(n) = \frac{1}{n!} \left(\frac{k_2\,\nu^2}{k_1\,B_0} \right)^n \exp\left[-\frac{k_2\,\nu^2}{k_1\,B_0} \right], \qquad n = 0, 1, 2, 3, \dots, \tag{3}$$

where B_0 is the (constant) number of molecules of B in the container. The results given by the formula (3) are plotted in Figure 1(b) as the circles. We confirm that the stationary distribution $\phi(n)$ is indeed given by (3). In what follows, we will use the stationary distributions of model problems to study the limitations of different stochastic reaction-diffusion methods. The average number of molecules of A in the container is given by (see Appendix A)

$$M_s = \frac{k_2\,\nu^2}{k_1\,B_0}. \tag{4}$$

Using the parameter values of Figure 1, we obtain $M_s = 5$. This number is plotted in Figure 1(a) as the dashed line. The variance of the Poisson distribution (3) is equal to its mean M_s.

2.2. A homoreaction example

Let us consider chemical species A and B in a container of volume ν which are subject to the following two chemical reactions

$$A + A \xrightarrow{k_1} B, \qquad\qquad \emptyset \xrightarrow{k_2} A. \tag{5}$$
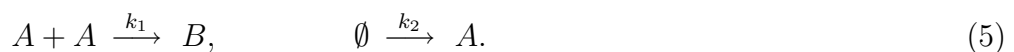
The first reaction describes the dimerization of the chemical A with the rate constant k_1. We couple it with the second reaction which represents the production of the chemical A with the rate constant k_2. This reaction has been already studied in the example (1). In what follows, we will only be interested in the time evolution and stationary distribution of A. The dynamics of the model (5) is similar to (1): some molecules of A are produced by the second reaction and some are removed by the first reaction. Thus, $A(t)$ fluctuates around its equilibrium value in a similar way as the trajectory in Figure 1(a) which has been computed for the heteroreaction example (1). If the reactor is well-stirred, the propensity functions of chemical reactions (5) are given by

$$\alpha_1(t) = A(t)(A(t) - 1)k_1/\nu, \qquad \alpha_2(t) = k_2\nu, \tag{6}$$

i.e. the probability that the i-th reaction in (5) occurs in the infinitesimally small time interval $[t, t + \mathrm{d}t)$ is $\alpha_i(t)\,\mathrm{d}t$, $i = 1, 2$. If the first chemical reaction occurs, then two molecules of A are removed from the system; if the second chemical reaction takes place, then one molecule of A is added to the system. This uniquely specifies the stochastic model as a Markov chain which can be simulated by the Gillespie SSA. The stationary distribution of (5) is given by (see Appendix A)

$$\phi(n) = \frac{C}{n!} \left(\frac{k_2\nu^2}{k_1}\right)^n I_{n-1}\left(2\sqrt{\frac{k_2\nu^2}{k_1}}\right), \qquad n = 0, 1, 2, 3, \ldots, \tag{7}$$

where I_n is the modified Bessel function of the first kind (see Glossary) and C is a positive constant given by the normalization $\sum_n \phi(n) = 1$. The average number of molecules of A in the container is given by (see Appendix A)

$$M_s = \frac{1}{4} + \sqrt{\frac{k_2\nu^2}{2k_1}}\, I_1'\left(2\sqrt{\frac{2k_2\nu^2}{k_1}}\right)\left[I_1\left(2\sqrt{\frac{2k_2\nu^2}{k_1}}\right)\right]^{-1}. \tag{8}$$

In Appendix A, we show that the stationary number of molecules of A obtained by the standard ordinary differential equation (ODE) model of the chemical system (5) is $\overline{A}_s = \nu\sqrt{k_2/(2k_1)}$. Note that this is not in general equal to M_s given by formula (8). For example, in the following section, we use the parameter values $k_1/\nu = 0.2\,\mathrm{sec}^{-1}$ and $k_2\nu = 10\,\mathrm{sec}^{-1}$. Then $\overline{A}_s = 5$ and $M_s \doteq 5.13$, i.e. the deterministic ODE does not provide the exact description of the stochastic mean. On the other hand, the difference between M_s and $\overline{A}_s$ is only 2.5% so that the ODE model gives a reasonable approximation of M_s. However, the comparison of deterministic and stochastic modelling is not the focus of this paper. Our main goal is to highlight some limitations of current reaction-diffusion SSAs and present improvements of these models. Examples of chemical systems where the differences between the results of stochastic simulation and the corresponding deterministic approximation (ODEs) are significant can be found in [31, 16, 7, 15].
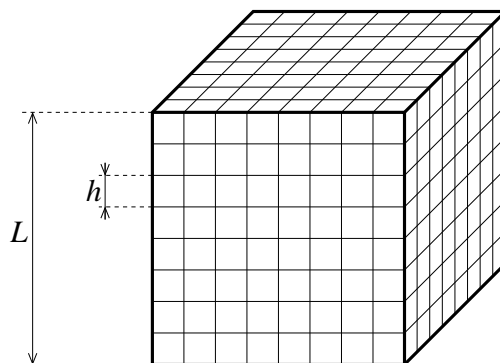
Figure 2. *Domain $[0, L] \times [0, L] \times [0, L]$ is divided into K^3 compartments of the volume $h^3 = (L/K)^3$. The division of the domain for $K = 8$ is shown on the picture.*

3. Disadvantages of current SSAs for reaction-diffusion modelling

In Section 2, we considered the illustrative examples (1) and (5) as well-stirred chemical systems. In particular, their mathematical models did not explicitly involve a description of molecular diffusion. In this section, we couple chemical systems (1) and (5) with models of molecular diffusion and show key limitations of reaction-diffusion SSAs in the literature. In what follows, we assume that chemical species A and B diffuse with diffusion constants D_A and D_B, respectively, in the cubic container $[0, L] \times [0, L] \times [0, L]$. We consider zero-flux (reflective) boundary conditions, i.e. whenever a molecule hits the boundary, it is reflected back. The implementation of more complicated (reactive) boundary conditions was studied in our previous paper [13].

3.1. Compartment-based model

In the compartment-based model, we divide the computational domain into small compartments which are assumed to be well-mixed. We postulate that only molecules in the same compartment can react according to bimolecular reactions. Diffusion is modelled as jumps of molecules between neighbouring compartments [24, 27].

Let us consider the heteroreaction example (1). We divide the cubic domain $[0, L] \times [0, L] \times [0, L]$ into K^3 cubic compartments of volume h^3 where $K \geq 1$ and $h = L/K$ (see Figure 2). In general, the compartment-based model can be formulated for compartments which are not cubic and which are not of the same size [27, 12]. However, for the purposes of this paper, it is sufficient to work with cubic compartments of the same size. They are the most natural choice, and are easy to implement computationally. Moreover, if the modeller does not use the uniform cubic mesh, it might be sometimes difficult to distinguish which results show a genuine property of the system and which are a consequence of the non-uniform mesh. Note that the uniform cubic mesh introduces an artificial anisotropy in the domain (e.g. compartments have different lengths along the side and along the diagonal). However, we will not explore potential consequences

of this anisotropy in this paper. We will focus on the more fundamental problem: the appropriate choice of compartment size h.

To precisely formulate the compartment-based SSA for the illustrative chemical system (1) in the reactor $[0, L] \times [0, L] \times [0, L]$, we denote the compartments by indices from the set

$$I_{all} = \{(i, j, k) \,|\, i, j, k \text{ are integers such that } 1 \leq i, j, k \leq K\}.$$
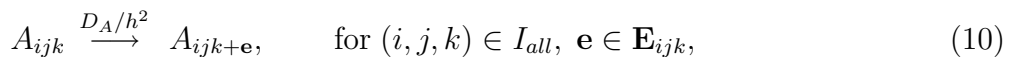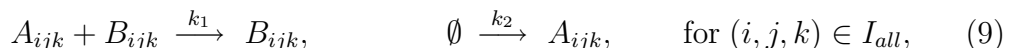
Let $A_{ijk}(t)$ (resp. $B_{ijk}(t)$) be the number of molecules of the chemical species A (resp. B) in the (i, j, k)-th compartment at time t where $(i, j, k) \in I_{all}$. Diffusion is modelled as a jump process between neighbouring compartments. Let us define the set of possible directions of jumps

$$\mathbf{E} = \{[1, 0, 0], \ [-1, 0, 0], \ [0, 1, 0], \ [0, -1, 0], \ [0, 0, 1], \ [0, 0, -1]\}.$$

For every $(i, j, k) \in I_{all}$, we also define

$$\mathbf{E}_{ijk} = \{\mathbf{e} \in \mathbf{E} \,|\, ((i, j, k) + \mathbf{e}) \in I_{all}\},$$

i.e $\mathbf{E}_{ijk}$ is the set of possible directions of jumps from the (i, j, k)-th compartment. The compartment-based reaction-diffusion model can be written using the chemical reactions formalism as follows. We study a system of $2K^3$ "chemical species" A_{ijk} and B_{ijk} for $(i, j, k) \in I_{all}$ which are subject to the chemical reactions:

$$A_{ijk} + B_{ijk} \ \xrightarrow{k_1} \ B_{ijk}, \qquad\qquad \emptyset \ \xrightarrow{k_2} \ A_{ijk}, \qquad \text{for } (i, j, k) \in I_{all}, \qquad (9)$$

$$A_{ijk} \ \xrightarrow{D_A/h^2} \ A_{ijk+\mathbf{e}}, \qquad \text{for } (i, j, k) \in I_{all}, \ \mathbf{e} \in \mathbf{E}_{ijk}, \qquad (10)$$

$$B_{ijk} \ \xrightarrow{D_B/h^2} \ B_{ijk+\mathbf{e}}, \qquad \text{for } (i, j, k) \in I_{all}, \ \mathbf{e} \in \mathbf{E}_{ijk}. \qquad (11)$$

The chemical reactions (9) correspond to the chemical system (1) considered in each compartment. It is assumed that each compartment is effectively well-stirred. A molecules of A and a molecule of B which are in the same compartment can react according to the bimolecular reaction $A + B \rightarrow B$. On the other hand, two molecules in different compartments cannot react with each other. The propensity functions of reactions (9) are

$$\alpha_{ijk,1}(t) = A_{ijk}(t) B_{ijk}(t) \, k_1/h^3, \qquad \alpha_{ijk,2}(t) = k_2 h^3 \qquad (12)$$

where h^3 is the volume of the compartment. The propensity functions (12) can be derived using the same argument as (2), replacing the volume $\nu = L^3$ of the whole reactor by the compartment volume h^3. The reactions (10)–(11) correspond to diffusive jumps between neighbouring compartments. The propensity functions of these "reactions" are equal to $A_{ijk}(t) \, D_A/h^2$ and $B_{ijk}(t) \, D_B/h^2$. There are $2K^3$ reactions in (9), $6K^3 - 6K^2$ diffusion "reactions" in (10) and $6K^3 - 6K^2$ diffusion "reactions" in (11) because there are 6 possible directions to jump from each inner compartment and some directions are missing for boundary compartments. Thus we are able to formulate the compartment-based reaction-diffusion model as the chemical system of $2K^3$ chemical species A_{ijk} and B_{ijk} which are subject to $14K^3 - 12K^2$ reactions (9)–(11). The time evolution
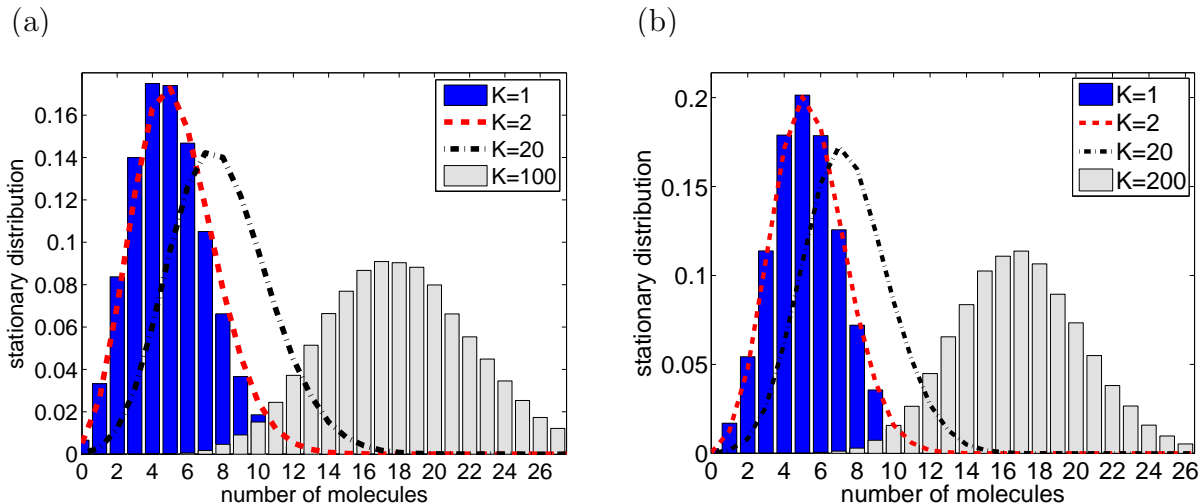
(a)   (b)

Figure 3. (a) *Heteroreaction example* (1). *Stationary distribution* $\phi_K(n)$, *defined by* (13) *and computed for* $K = 1, 2, 20$, *and* 100 *by long time simulations of the Gillespie SSA. We use* $k_1 = 0.2\ \mu\text{m}^3\ \text{sec}^{-1}$, $k_2 = 1\ \mu\text{m}^{-3}\ \text{sec}^{-1}$, $D_A = D_B = 1\ \mu\text{m}^2\ \text{sec}^{-1}$, $L = 1\ \mu\text{m}$ *and* $B_0 = 1$. (b) *Homoreaction example* (5). *Stationary distribution* $\phi_K(n)$ *for* $K = 1, 2, 20$, *and* 200 *computed by long time simulations of the Gillespie SSA. We use* $k_1 = 0.2\ \mu\text{m}^3\ \text{sec}^{-1}$, $k_2 = 10\ \mu\text{m}^{-3}\ \text{sec}^{-1}$, $D_A = 1\ \mu\text{m}^2\ \text{sec}^{-1}$ *and* $L = 1\ \mu\text{m}$.

of the chemical system (9)–(11) can be simulated by the Gillespie SSA. It can be also equivalently described in terms of the reaction-diffusion master equation, which is given in Appendix B as equation (B.2). The number of molecules of A in the whole container $[0, L] \times [0, L] \times [0, L]$ is given by

$$A(t) = \sum_{(i,j,k) \in I_{all}} A_{ijk}(t).$$

Let $p_n(t)$ be the probability that $A(t) = n$. Let $\phi_K(n)$ be the stationary distribution defined by (compare with (A.2))

$$\phi_K(n) = \lim_{t \to \infty} p_n(t). \tag{13}$$

Thus, $\phi_K(n)$ is the probability that there are n molecules of A in the system, provided that the system is observed for long time. In particular, $\phi_1(n)$ is equal to the stationary distribution $\phi(n)$ given by (3). Since production of A is homogeneous throughout the container, we would expect the distribution of A to be uniform in space, so that we should find that ϕ_K is independent of K. In Figure 3(a), we present the stationary distributions $\phi_K(n)$ for $K = 1, 2, 20$ and 100 for the parameter values $L = 1\ \mu\text{m}$, $D_A = D_B = 1\ \mu\text{m}^2\ \text{sec}^{-1}$, $k_1 = 0.2\ \mu\text{m}^3\ \text{sec}^{-1}$, $k_2 = 1\ \mu\text{m}^{-3}\ \text{sec}^{-1}$ and $B_0 = 1$. In particular, we have the same rates for $K = 1$ as were used in Figure 1, namely $k_1/L^3 = 0.2\ \text{sec}^{-1}$ and $k_2 L^3 = 1\ \text{sec}^{-1}$. Thus the stationary distribution $\phi_1(n)$, plotted in Figure 3(a), is equal to the distribution $\phi(n)$ plotted in Figure 1(b).

Increasing K (i.e. decreasing h), the stationary distribution $\phi_K(n)$ moves to the right. The shift to the right is in agreement with the result of Isaacson [26] who showed that, in the theoretical limit $h \to 0$, the bimolecular reaction $A + B \to \emptyset$ is lost and

the compartment-based modelling of this reaction only recovers the diffusion process. In our case, we coupled the bimolecular reaction with the production of A molecules. The production rate per the whole domain is equal to

$$\sum_{(i,j,k)\in I_{all}} \alpha_{ijk,2}(t) = \sum_{(i,j,k)\in I_{all}} k_2 h^3 = K^3 k_2 h^3 = k_2 L^3,$$

i.e. it is independent of h. Thus, for small h, the slower removal of A by the bimolecular reaction and unchanged production rate of A result in the shift of the stationary distribution $\phi_K(n)$ to the right in Figure 3(a), as K is increased (i.e. as $h = L/K$ is decreased). In Figure 3(b), we present the results of a similar computation for the homoreaction example (5). In this case, the homodimerization $A + A \rightarrow B$ is replaced by K^3 reactions $A_{ijk} + A_{ijk} \rightarrow B_{ijk}$ for $(i,j,k) \in I_{all}$. The propensity functions of these reactions are given by

$$\alpha_{ijk,1}(t) = A_{ijk}(t)(A_{ijk}(t) - 1)\, k_1/h^3. \tag{14}$$

The production reaction and diffusion are treated as in (9)–(10). In Figure 3(b), we present the stationary distributions $\phi_K(n)$ for four values of K. Notice that $\phi_1(n)$ is equal to the stationary distribution $\phi(n)$ given by (7). We observe the same phenomenon (shift of the histogram to the right) as in the case of the heteroreaction example.

Although it is generally agreed in the literature that there is a bound on h from below [27, 26], this bound is usually stated in the form $h \gg k_1/(D_A + D_B)$ or $h \gg \varrho$ where ϱ is the binding radius for the molecular based Smoluchowski model – see equation (21) and the discussion in Section 3.2. To satisfy these conditions in our particular example, we could simply choose $h = L$. However, the real importance of stochastic reaction-diffusion modelling is not in modelling of spatially homogeneous systems. If the system has some spatial variations (i.e. some parts of the computational domain are more preferred by molecules than the others), then we obviously want to choose h small enough to capture the desired spatial resolution. This leads to the restriction on h from above, namely $L \gg h$. Thus it is suggested to choose h small (to satisfy $L \gg h$) but not too small (to satisfy $h \gg k_1/(D_A + D_B)$) [27] which leads to the important question what the optimal choice of h should be to get the most accurate results. In this paper, we propose a different route to this problem. In Section 4.1, we show that there exists a critical value h_{crit} such that the propensity function of the compartment-based model can be adjusted for $h \geq h_{crit}$ to recover correctly the stationary distribution $\phi(n)$. Thus we effectively replace the condition $h \gg k_1/(D_A + D_B)$, which requires that h is much larger than $k_1/(D_A + D_B)$ by a sharp inequality $h \geq h_{crit}$, where h_{crit} is approximately a quarter of $k_1/(D_A + D_B)$. We will show that the compartment-based model can be appropriately modified to correctly simulate chemical systems for any $h \geq h_{crit}$. In particular, we also get a measure of correctness of the original compartment-based model.

3.2. Molecular-based models

In this section, we study molecular-based models of reaction-diffusion processes, i.e. we simulate trajectories of individual molecules. The position $[X(t), Y(t), Z(t)]$ of a diffusing molecule (Brownian motion) can be described by a system of three (uncoupled) stochastic differential equations (SDEs) [6]

$$X(t + \mathrm{d}t) = X(t) + \sqrt{2D}\, \mathrm{d}W_x, \tag{15}$$

$$Y(t + \mathrm{d}t) = Y(t) + \sqrt{2D}\, \mathrm{d}W_y, \tag{16}$$

$$Z(t + \mathrm{d}t) = Z(t) + \sqrt{2D}\, \mathrm{d}W_z, \tag{17}$$

where $\mathrm{d}W_x$, $\mathrm{d}W_y$, $\mathrm{d}W_z$ are (uncorrelated) white noises (i.e. differentials of the Wiener process) and D is the diffusion constant. To simulate trajectories of the system of SDEs (15)–(17), we choose a small time step Δt and use the Euler-Maruyama method [25] to solve SDEs (15)–(17); that is, we compute the position $[X(t + \Delta t), Y(t + \Delta t), Z(t + \Delta t)]$ at time $t + \Delta t$ from its position $[X(t), Y(t), Z(t)]$ at time t by

$$X(t + \Delta t) = X(t) + \sqrt{2D\Delta t}\, \xi_x, \tag{18}$$

$$Y(t + \Delta t) = Y(t) + \sqrt{2D\Delta t}\, \xi_y, \tag{19}$$

$$Z(t + \Delta t) = Z(t) + \sqrt{2D\Delta t}\, \xi_z, \tag{20}$$

where D is the diffusion constant and ξ_x, ξ_y, ξ_z are random numbers which are sampled from the normal distribution with zero mean and unit variance. To model a bimolecular reaction, it is often postulated that two molecules (which are subject to the bimolecular reaction) always react whenever their distance is less than a given reaction radius ϱ [33, 3]. If trajectories of molecules exactly follow the system of SDEs (15)–(17), one can find explicit formulae linking the reaction rate constant, the diffusion constant(s) of reactants and the reaction radius [33, 5, 4]. The reaction radius of heteroreaction (1) is

$$\varrho = \frac{k_1}{4\pi(D_A + D_B)} \tag{21}$$

and the reaction radius of homoreaction (5) is $k_1/(4\pi D_A)$. Thus, the illustrative example (1) can be simulated as follows. We choose a small time step Δt. We update the position of every molecule by (18)–(20) where $D = D_A$ for molecules of A and $D = D_B$ for molecules of B. Reflecting boundary conditions are implemented on the boundary of the cubic computational domain $[0, L] \times [0, L] \times [0, L]$. For example, if $X(t + \Delta t)$ computed by (18) is less than 0, then $X(t + \Delta t) = -X(t) - \sqrt{2D\,\Delta t}\, \xi_x$. If $X(t + \Delta t)$ computed by (18) is greater than L, then $X(t + \Delta t) = 2L - X(t) - \sqrt{2D\,\Delta t}\, \xi_x$. Similarly for y and z-coordinates. Whenever the distance of a molecule of A from a molecule of B is less than the reaction radius ϱ given by (21), we remove the molecule of A from the system. We also generate a random number r uniformly distributed in $(0, 1)$ during every time step. If $r < k_2 L^3 \Delta t$, then we generate another three random numbers r_x, r_y and r_z uniformly distributed in $(0, 1)$ and introduce a new molecule of A at the position $(r_x L, r_y L, r_z L)$.

Having explained the most straightforward implementation of a molecular-based model, we now highlight some of its problems. First of all, the diffusing molecule was

described by the vector $[X(t), Y(t), Z(t)]$ of its position. This means that we effectively modelled the diffusing molecule as a point-like particle, ignoring its three-dimensional structure. To get some insights into the validity of this assumption, let us consider that the diffusing molecule is a protein. Then the typical values of its molecular radius are between 1 and 5 nanometres [1]. It is illustrative to compare the molecular radius with the reaction radius ϱ given by (21). Using the typical parameter values for interactions between proteins [30] (i.e. $k_1 = 10^6 \, \mathrm{M}^{-1} \sec^{-1}$ and $D_A = D_B = 10^{-6} \, \mathrm{cm}^2 \sec^{-1}$), we obtain $\varrho = 0.02$ nm. Thus the reaction radius ϱ given by (21) is unrealistically smaller than the molecular radius. Obviously, if we interpret the position vector $[X(t), Y(t), Z(t)]$ as the center of the hard sphere of the molecular radius ϱ_m, then two spheres will never get closer than ϱ_m. Consequently, the relation $\varrho \ll \varrho_m$ makes the molecular-based model unrealistic at the level of individual molecules. It is worth noting that this undesirable property of the model does not depend on the value of the diffusion constant D. This can be seen as follows. Approximating the diffusing molecule as a sphere, we can estimate its radius by the Stokes-Einstein relation [10, 4]

$$\varrho_m = \frac{k_B T}{6\pi \eta D},\tag{22}$$

where $k_B = 1.38 \times 10^{-14} \, \mathrm{g \, mm^2 \, sec^{-2} \, K^{-1}}$ is the Boltzmann constant, T is the absolute temperature, η is the coefficient of viscosity and D is the diffusion constant. Let us investigate the conditions under which the reaction radius ϱ is smaller than the molecular radius ϱ_m. Using (22), (21) and $D = D_A = D_B$, the inequality $\varrho < \varrho_m$ is equivalent to

$$k_1 < \frac{4k_B T}{3\eta}.$$

Considering a solution in water or in the fluid-phase of cytoplasm ($\eta \approx 10^{-3} \, \mathrm{g \, mm^{-1} \, sec^{-1}}$ [20]) at room temperature ($T \approx 300 \, \mathrm{K}$), we see that the inequality $\varrho < \varrho_m$ is satisfied for values of k_1 up to the order $10^8 \, \mathrm{M}^{-1} \sec^{-1}$. Typical values of k_1 for interactions between proteins are of the order $10^6 \, \mathrm{M}^{-1} \sec^{-1}$ [30]. Thus, unless the reaction rate constant k_1 is very large, the model requires the reaction radius ϱ to be chosen unrealistically small.

Perhaps more importantly, a small reaction radius also provides restrictions on the simulation time step Δt. We have to make sure that the average change in the distance between molecules during one time step is much less than the reaction radius ϱ. Following [3], we formulate this condition as $s \ll \varrho$, where s is the root mean square step length (in each coordinate) given by

$$s = \sqrt{2(D_A + D_B)\Delta t}.\tag{23}$$

Using $D_A = D_B = 10 \, \mu\mathrm{m}^2 \, \sec^{-1}$ and $k_1 = 10^6 \, \mathrm{M}^{-1} \sec^{-1}$, we obtain that Δt has to be significantly less than a nanosecond. This limitation is even more severe for faster diffusing molecules.* The bimolecular reaction can, in principle, be simulated with a very large time step Δt but the formula for ϱ has to be modified accordingly. If

---

* As the illustrative model is formulated, we also have to make sure that the production probability per one time step, $k_2 L^3 \Delta t$, is significantly less than 1. This is indeed the case for all simulations presented.

$s \gg \varrho$, then the probability that a given pair of molecules interacts during the time step $(t, t + \Delta t)$ is proportional to the volume fraction $4\pi\varrho_\infty^3/(3L^3)$ where ϱ_∞ is the modified reaction radius. Comparing with $k_1 \Delta t/L^3$, we obtain [3]

$$\varrho_\infty = \left(\frac{3k_1 \Delta t}{4\pi}\right)^{1/3}. \tag{24}$$

This formula gives a larger (Δt-dependent) reaction radius, but it does not have the potential to provide a spatial resolution close to the size of individual molecules. Andrews and Bray [3] designed a computational algorithm for intermediate values of Δt that satisfies $s \approx \varrho$. In this case, it is not possible to derive an explicit formula relating ϱ and k_1 (as was done in (21) for $s \ll \varrho$ and in (24) for $s \gg \varrho$). Instead Andrews and Bray [3] provide a look-up table relating (scaled) reaction rate constant k_1 and reaction radius ϱ. However, the reaction radius is still often smaller than molecular radius ϱ_m in their algorithm. In Section 4.2, we will modify molecular-based algorithms so that the reaction radius can be chosen as large as the molecular radius. Let us note that the algorithms above consider all "collisions" of reactants as reactive while in reality many non-reactive collisions happen before the reaction takes place. The modified algorithms in Section 4.2 take this point into account.

4. Improved SSAs for reaction-diffusion modelling

In this section, we present modified SSAs which are able to overcome the problems mentioned in Section 3. To make this section accessible to non-mathematicians, we focus only on the results. The mathematical derivation of the formulae presented and the justification of the modified algorithms are given in Appendices.

4.1. Improved compartment-based model

Let us consider the heteroreaction example (1) modelled by the compartment-based reaction-diffusion model (9)–(11). We will show that a suitable modification of propensity functions $\alpha_{ijk,1}(t)$, which were defined by (12), leads to an algorithm that gives the correct $\phi(n)$ for any h larger than or equal to the critical value h_{crit}. Moreover, this is not possible for values of h smaller than h_{crit}. The critical value of the compartment size h can be estimated as

$$h_{crit} = \beta_\infty \frac{k_1}{D_A + D_B} \tag{25}$$

where k_1 is the rate constant of the bimolecular reaction, D_A (resp. D_B) is the diffusion constant of A (resp. B) and $\beta_\infty \approx 0.25272$. If h_{crit} computed by (25) is significantly smaller than the domain size L, then the critical value of h is indeed given by (25). If the domain size L is comparable to (25), then (25) provides only a good approximation

However, it is worth noting that the production (which is the zero-order reaction) does not limit the time step. If $k_2 L^3 \Delta t$ is large, one can add more molecules per time step using a Poisson-distributed random number [3].

K	β	K	β	K	β	K	β
2	0.30208	9	0.31406	25	0.28514	150	0.26103
3	0.33233	10	0.31067	30	0.28123	200	0.25930
4	0.33461	12	0.30493	40	0.27587	300	0.25743
5	0.33119	14	0.30027	50	0.27232	400	0.25643
6	0.32660	16	0.29643	60	0.26979	600	0.25536
7	0.32205	18	0.29322	80	0.26640	800	0.25479
8	0.31784	20	0.29048	100	0.26420	1000	0.25443

Table 1. *The values of β for the selected values of K computed by* (27) *for the heteroreaction example* (1) *for $B_0 = 1$.*

of h_{crit}, with the real value being slightly higher as discussed below. If $h \geq h_{crit}$, we propose to modify the first formula in (12) by

$$\alpha_{ijk,1}(t) = A_{ijk}(t)B_{ijk}(t) \frac{(D_A + D_B)k_1}{(D_A + D_B)h^3 - \beta k_1 h^2} \tag{26}$$

where the parameter β has no physical dimension and needs to be specified. If a modeller does not have any information about the system, we propose to choose $\beta = \beta_\infty \approx 0.25272$. We will show later that β_∞ is indeed the correct choice of β if $K = L/h$ is large. Formula (26) can be applied to any heteroreaction $A + B \to \emptyset$ where $\emptyset$ stands for an arbitrary right hand side, provided that the propensity function (26) is positive. Consequently, the critical value h_{crit} is the one which makes the denominator of (26) equal to zero. In such a case, the propensity function is infinity and the reaction happens immediately after the reacting molecules enter the same compartment. Thus, h_{crit} satisfies $(D_A + D_B)h_{crit}^3 - \beta h_{crit}^2 k_1 = 0$. If we substitute β_∞ for β, we obtain the approximation (25).

Let us consider the illustrative heteroreaction example plotted in Figure 3(a). The values of the constant β for this model are given for different values of K in Table 1, and lie between $\beta_\infty \approx 0.25272$ and 0.34. Increasing K to infinity, the values of β converge to β_∞. In Figure 4(a), we compare the results computed using the original formula (12) and by the new formula (26) for the heteroreaction example (1). We use the same parameter values as in Figure 3(a) and $K = 16$. As in Figure 3(a), we observe a difference between $\phi_1(n)$ and $\phi_{16}(n)$ if the original model is used. On the other hand, $\phi_{16}(n)$ computed by the modified algorithm (solid line) is the same as $\phi_1(n)$ (grey histogram).

In Table 1, we observe that β weakly depends on $K = L/h$, so that the real value of h_{crit} (that makes the propensity function (26) equal to infinity) is slightly larger than (25). The dependence of β on K is caused by the boundary of the computational domain $[0, L] \times [0, L] \times [0, L]$. Every inner compartment can be entered from six possible directions, but some incoming directions are missing in the boundary compartments. Whenever a molecule of B is in a boundary compartment, it is less likely found by molecules of A. One could address this problem either by introducing different propensity functions for different compartments, or by using β in (26) which is slightly

larger than β_∞. We used the latter option. In Appendix C, we show that the modified β is given by

$$\beta = \frac{1}{2K^3} \sum_{\substack{i,j,k=0 \\ (i,j,k) \neq (0,0,0)}}^{K-1} \frac{1}{3 - \cos(i\pi/K) - \cos(j\pi/K) - \cos(k\pi/K)}. \tag{27}$$

The results in Table 1 have been computed by (27). In Appendix D, we show that β_∞ is given by

$$\beta_\infty = \frac{1}{2\pi^2} \int_0^\pi \int_0^\pi \frac{1}{\sqrt{(3 - \cos x - \cos y)^2 - 1}} \, \mathrm{d}x \, \mathrm{d}y. \tag{28}$$

Evaluating this integral numerically by the Monte Carlo method, we obtain $\beta_\infty \approx 0.25272$. If we model a complicated reaction-diffusion system, modelling of each heteroreaction will be improved by using (26), provided that all rates obtained by (26) are positive. In other words, the smallest possible h which can be simulated is given as the maximal h_{crit} for each bimolecular reaction. If h is significantly larger then h_{crit} (i.e. if $h \gg h_{crit}$), then we have $(D_A + D_B)h^3 \gg \beta k_1 h^2$ and we can approximate

$$\frac{(D_A + D_B)k_1}{(D_A + D_B)h^3 - \beta k_1 h^2} \approx \frac{k_1}{h^3}. \tag{29}$$

In particular, the propensity function $\alpha_{ijk,1}(t)$ defined by (26) is approximately equal to the original propensity function (12) for large values of h. On the other hand, if h is close to h_{crit}, then the propensity function $\alpha_{ijk,1}(t)$ given by (26) is larger than the original propensity function (12).

Finally, let us consider the homoreaction example (5) modelled by the compartment-based model. In this case, we propose to modify the propensity functions (14) for $h \geq h_{crit}$, by $\alpha_{ijk,1}(t)$

$$\alpha_{ijk,1}(t) = A_{ijk}(t)(A_{ijk}(t) - 1) \frac{D_A k_1}{D_A h^3 - \beta k_1 h^2}, \tag{30}$$

where β is a constant. In Figure 4(b), we compare the results computed using the original formula (14) and by the new formula (30) for the value of β given by Table 1. We use the same parameter values as in Figure 3(b) and $K = 16$. We again observe that the modified formula (30) gives better results than the original SSA. One can still observe a small error which is caused by the fact that we used the value of β computed for heteroreactions. Using (27), we have $\beta \approx 0.29643$ for $K = 16$ (see Table 1). Experimenting with the model (5), we can find that $\beta = 0.28$ yields slightly better fit between $\phi_1(n)$ and $\phi_{16}(n)$. Notice that $\beta = 0.28$ is still larger than $\beta_\infty \approx 0.25272$. However, for the purposes of applications, it is sufficient to use either $\beta = \beta_\infty$ or the values of β from Table 1 for both heteroreactions and homoreactions. Using $\beta = \beta_\infty$, we discovered that the biggest contribution of the error stems from the boundary effects and derived Table 1 which adds a correction to β_∞ to compensate for boundary behaviour. In a similar way, one could look for further corrections to the value of β for homoreactions, or for domains which are cuboids rather than cubes. Although such corrections are of
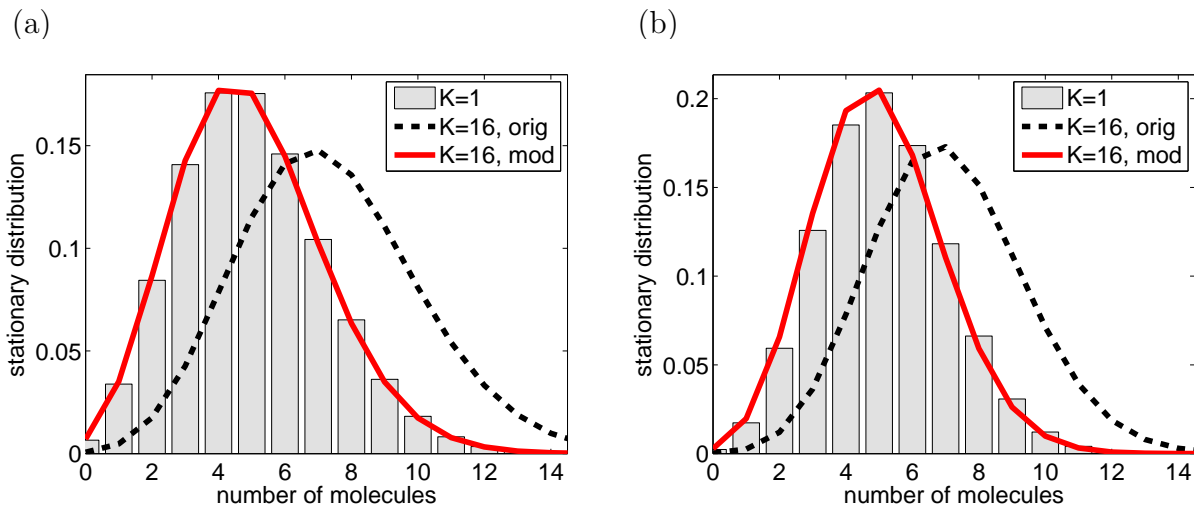
Figure 4. (a) *Heteroreaction example* (1). *Stationary distribution* $\phi_{16}(n)$ *defined by* (13) *computed by the original SSA (dashed line) and by the modified SSA that uses* (26) *instead of* (12) *(solid line). Correct stationary distribution* $\phi(n) \equiv \phi_1(n)$ *is plotted as the grey histogram.* (b) *Homoreaction example* (5). *Stationary distribution* $\phi_{16}(n)$ *computed by the original SSA (dashed line) and by the modified SSA that uses* (30) *instead of* (14) *(solid line). Correct stationary distribution* $\phi(n) \equiv \phi_1(n)$ *is plotted as the grey histogram.*

interest from the mathematical point of view, they provide only a negligible improvement of the algorithm. Thus we will not include them in this paper.

4.2. Improved molecular-based models

The major assumption of molecular-based models is that molecules always react whenever their distance is less than the reaction radius ϱ. The reaction radius ϱ is related to the rate constant of the bimolecular reaction by a simple formula (for example, (21) for the Smoluchowski model) or by a look up table for the Andrews and Bray model [3]. In this section, we present models that implement bimolecular reactions with the help of two parameters: the reaction radius $\bar{\varrho}$ and the reaction rate λ. We postulate that the bimolecular reaction can take place only when the distance of molecules is less than $\bar{\varrho}$. If this is the case, then the bimolecular reaction events happen with the rate λ. We will call this model $\lambda - \bar{\varrho}$ model in what follows.

To implement this idea on the computer, we need to relate the parameters λ and $\bar{\varrho}$ to the rate constant of the bimolecular reaction. The advantage of the $\lambda - \bar{\varrho}$ model is that many different pairs of λ and $\bar{\varrho}$ correspond to the same bimolecular rate constant. In mathematical terms, the condition on λ and $\bar{\varrho}$ is one equation for two unknowns λ and $\bar{\varrho}$. In particular, we can choose the value of $\bar{\varrho}$ as desired (e.g. to be comparable to the molecular radius ϱ_m) and compute the appropriate value of λ. Thus $\lambda - \bar{\varrho}$ model has the potential to solve the problems of molecular-based modelling discussed in Section 3.2.

We explain the $\lambda - \bar{\varrho}$ model on the heteroreaction example (1). The diffusion of

molecules A and B is simulated as in Section 3.2. We choose a small time step Δt. The trajectory of every molecule is computed by (18)–(20) where $D = D_A$ for molecules of A and $D = D_B$ for molecules of B. Let s be given by (23). We will distinguish two cases of the value of the time step: (i) the time step Δt is chosen so small that $s \ll \overline{\varrho}$; and (ii) the time step Δt is larger so that $s \approx \overline{\varrho}$.

(i) Small time step Δt. To model heteroreaction $A + B \to \cdots$, we introduce two parameters: reaction radius $\overline{\varrho}$ and rate λ. The reaction radius is expressed in units of length and rate λ in units per time. Whenever the distance of a molecule of A from a molecule of B is less than the reaction radius $\overline{\varrho}$, then the heteroreaction takes place with the rate λ. In Appendix E, we derive the following relation between $\overline{\varrho}$, λ and the rate constant k_1 of the heteroreaction:

$$k_1 = 4\pi(D_A + D_B)\left(\overline{\varrho} - \sqrt{\frac{D_A + D_B}{\lambda}} \tanh\left(\overline{\varrho}\sqrt{\frac{\lambda}{D_A + D_B}}\right)\right). \qquad (31)$$

This is one condition for two unknowns $\overline{\varrho}$ and λ. In particular, we can choose $\overline{\varrho}$ comparable to the radii of reacting molecules and use (31) to compute the corresponding λ. Notice that (31) is a simple non-linear equation which can be solved by any numerical method for finding roots of a real-valued function (for example, Newton's method or the bisection method).

If $\lambda = \infty$ (that is, if molecules react immediately whenever they are within the reaction radius), then (31) simplifies to (21) as desired. On the other hand, if λ is small that $\lambda \ll (D_A + D_B)/\overline{\varrho}^2$, then we can use Taylor expansion in (31) to approximate

$$\tanh\left(\overline{\varrho}\sqrt{\lambda/(D_A + D_B)}\right) \approx \overline{\varrho}\sqrt{\lambda/(D_A + D_B)} - \frac{1}{3}\left(\overline{\varrho}\sqrt{\lambda/(D_A + D_B)}\right)^3.$$

Consequently, (31) simplifies to $k_1 \approx 4\pi\overline{\varrho}^3\lambda/3$ which can be equivalently rewritten as

$$\lambda \approx \frac{k_1}{4\pi\overline{\varrho}^3/3}, \qquad (32)$$

i.e. the reaction rate λ is given as the reaction rate constant k_1 divided by the volume, $4\pi\overline{\varrho}^3/3$, of the ball in which the reaction takes place. Formula (32) is analogous to the formula for the reaction rate per compartment in the compartment-based approach for large compartment size h. If h is large satisfying $h \gg h_{crit}$, then the reaction rate per compartment is given as k_1/h^3, which is the reaction rate constant k_1 divided by the volume, h^3, of the compartment – see (29).

(ii) SSA for larger time steps. We introduce two parameters: reaction radius $\overline{\varrho}$ and probability P_λ. The heteroreaction $A + B \to \cdots$ is modelled as follows: whenever the distance between a molecule of A and a molecule of B (at the end of a time step) is less than the reaction radius $\overline{\varrho}$, then the heteroreaction takes place with probability P_λ; that is, we generate a random number r uniformly distributed in $(0, 1)$ and the heteroreaction (removal/addition of molecules) is performed whenever $r < P_\lambda$. Notice that the previous algorithm (for small time step Δt) can be also formulated in terms of parameters $\overline{\varrho}$ and P_λ rather than $\overline{\varrho}$ and λ. Indeed, if $\lambda \Delta t \ll 1$, we have $P_\lambda \approx \lambda \Delta t$. If Δt is larger, then

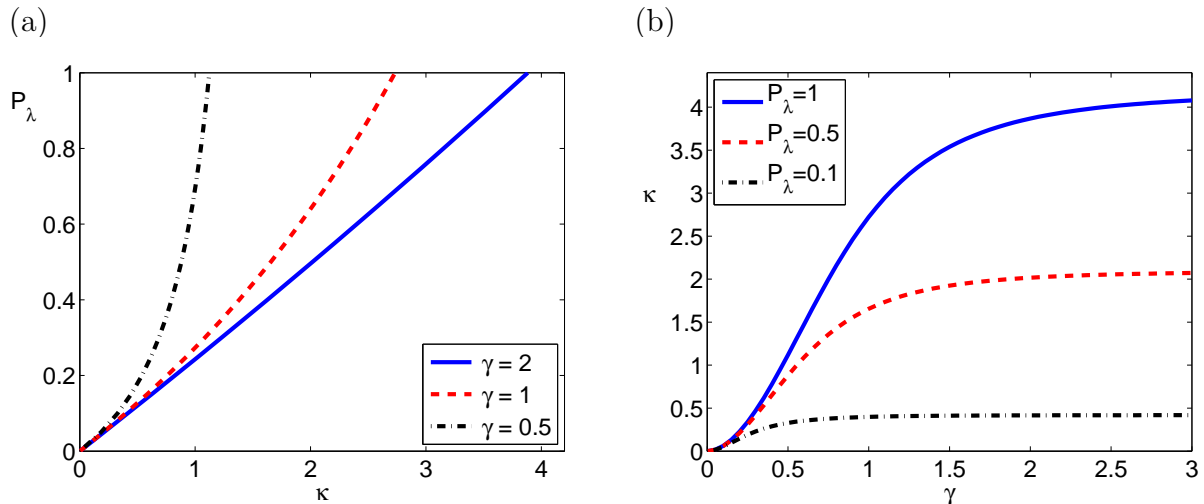(a)   (b)

Figure 5. (a) *Dependence of P_λ on κ for three different values of γ. Dimensionless parameters κ and γ are given by (33).* (b) *Dependence of κ on γ for three different values of P_λ.*

the relation between P_λ and λ is more complicated. However, from the practical point of view, there is no need to know the rate λ: it is sufficient to formulate the algorithms in terms of $\overline{\varrho}$ and P_λ. Next, we present the condition relating $\overline{\varrho}$ and P_λ with the rate constant k_1 of heteroreaction $A + B \to \cdots$. We define dimensionless parameters γ and κ by

$$\gamma = \frac{s}{\overline{\varrho}} = \frac{\sqrt{2(D_A + D_B)\Delta t}}{\overline{\varrho}}, \qquad\qquad \kappa = \frac{k_1\,\Delta t}{\overline{\varrho}^3}. \qquad (33)$$

In applications, we first specify the time step Δt. We also want to specify $\overline{\varrho}$ in a realistic parameter range. Consequently, γ and κ can be considered as given numbers in what follows. For example, we can choose the root mean square step length s equal to the reaction radius $\overline{\varrho}$. Then (33) gives $\gamma = 1$. The key modelling question is: what is the appropriate value of the probability P_λ? In Figure 5(a), we present the dependence of P_λ on κ for three different values of γ. The derivation of the equation for P_λ and the numerical method which was used to compute this plot are given in Appendix F. Below, we summarize only the equations that were solved and present illustrative computational results.

To formulate the equation for P_λ, it is useful to define an (auxiliary) function $g(r) : [0, \infty) \to [0, 1]$ as the solution of the integral equation

$$g(r) = (1 - P_\lambda) \int_0^1 K(r, r'; \gamma)\, g(r')\, dr' + \int_1^\infty K(r, r'; \gamma)\, g(r')\, dr', \qquad (34)$$

satisfying $g(r) \to 1$ as $r \to \infty$, where

$$K(r, r'; \gamma) = \frac{r'}{r\gamma\sqrt{2\pi}} \left(\exp\left[-\frac{(r - r')^2}{2\gamma^2} \right] - \exp\left[-\frac{(r + r')^2}{2\gamma^2} \right] \right). \qquad (35)$$

The function $g(r)$ depends on dimensionless parameters P_λ and γ; we make this explicit by writing

$$g(r; P_\lambda, \gamma) \equiv g(r).$$

Then, the model parameters $\bar{\varrho}$, P_λ, Δt are related to rate constant k_1 and diffusion constants D_A, D_B by

$$\kappa = P_\lambda \int_0^1 4\pi r^2 g(r; P_\lambda, \gamma) \, \mathrm{d}r. \tag{36}$$

Since k_1, D_A and D_B are known and parameters Δt and $\bar{\varrho}$ can be specified first, parameters γ and κ are in applications given numbers. Thus (36) is one equation for one unknown P_λ. In Appendix F, we present a numerical approach for solving this equation, as well as the derivation of (34)–(36).

In Figure 5(b), we present the dependence of κ on γ for three different values of P_λ. Note that the case $P_\lambda = 1$ corresponds to the Andrews and Bray model [3]. Thus the solid line in Figure 5(b) has been already computed in reference [3]. However, we propose to use a much smaller value of P_λ, which enables us to choose a larger (more physically meaningful) reaction radius. We see in Figure 5 that reducing P_λ at γ fixed corresponds to reducing κ, thereby increasing the reaction radius.

The heteroreaction example (1) is simulated by the $\lambda - \bar{\varrho}$ model as follows. We update the position of every molecule by (18)–(20) where $D = D_A$ for molecules of A and $D = D_B$ for molecules of B. Reflecting boundary conditions are implemented on the boundary of the cubic computational domain $[0, L] \times [0, L] \times [0, L]$ as in Section 3.2. The production of molecules of A (i.e. the second reaction in (1)) is simulated as before. We generate a random number r uniformly distributed on $[0, 1]$ during every time step. If $r < k_2 L^3 \Delta t$ ($\ll 1$), then we generate another three random numbers r_x, r_y and r_z uniformly distributed on $[0, 1]$ and introduce a new molecule of A at the position $(r_x L, r_y L, r_z L)$. If the separation between a molecule of A and a molecule of B (at the end of a time step) is less than the reaction radius $\bar{\varrho}$, then we generate a random number r uniformly distributed on $[0, 1]$ and we remove the molecule of A from the system if $r < P_\lambda$. In Figure 6(a), we present the stationary distribution computed by this algorithm (grey histogram). The value of P_λ, i.e $P_\lambda = 0.77\,\%$, was computed by solving (34)–(36) using the numerical method given in Appendix F. The values of parameters are given in the caption of Figure 6(a). Notice that the reaction radius is 40 nm and the time step Δt was chosen so that $\gamma = 0.5$. The comparison of computational results with formula (3) (solid line) is excellent.

Next, we consider the homoreaction example (5). Since two molecules of A are removed from the system whenever the homoreaction takes place, we have to replace k_1 by $2k_1$ in the above formulae. In particular, we replace κ by 2κ in (36). Moreover, $D_A + D_B$ has to be replaced by $2D_A$ in all formulae. Otherwise, method (34)–(36) for computing P_λ stays the same. In Figure 6(b), we present the stationary distribution computed by the λ-$\bar{\varrho}$ model (grey histogram). The comparison with exact formula (7) (solid line) is again excellent.
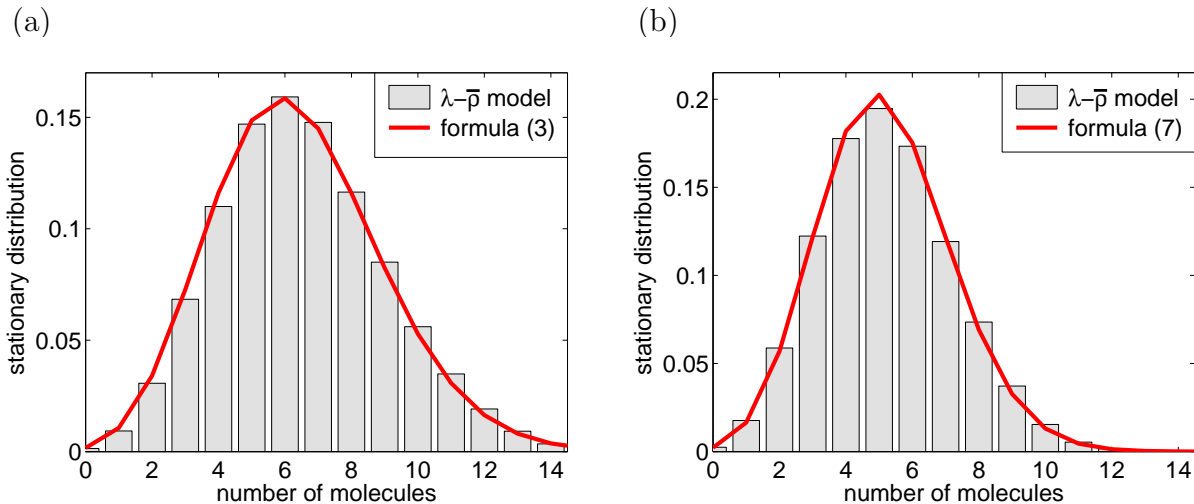
(a)
(b)

Figure 6. (a) *Heteroreaction example* (1). *Stationary distribution computed by the λ-$\bar{\varrho}$ model (grey histogram) and by formula* (3) *(solid line). We use $k_1 = 0.2\ \mu m^3\ sec^{-1}$, $k_2 = 0.02\ \mu m^{-3}\ sec^{-1}$, $D_A = D_B = 10\ \mu m^2\ sec^{-1}$, $L = 2\ \mu m$, $B_0 = 1$, $\Delta t = 10^{-5}\ sec$, $\bar{\varrho} = 40\ nm$ and $P_\lambda = 7.7 \times 10^{-3}$.* (b) *Homoreaction example* (5). *Stationary distribution computed by the λ-$\bar{\varrho}$ model (grey histogram) and by formula* (7) *(solid line). We use $k_1 = 0.1\ \mu m^3\ sec^{-1}$, $k_2 = 0.08\ \mu m^{-3}\ sec^{-1}$, $D_A = 10\ \mu m^2\ sec^{-1}$, $L = 2\ \mu m$, $\bar{\varrho} = 40\ nm$ and $P_\lambda = 7.7 \times 10^{-3}$.*

In this section, we focussed on the λ-$\bar{\varrho}$ model, which has been formulated in terms of two parameters – the reaction radius $\bar{\varrho}$ and the reaction probability P_λ. We showed that one parameter (P_λ) can be used to fit the macroscopic reaction rate constant, while the other parameter ($\bar{\varrho}$) can be used to get a more realistic fit with the microscopic molecular-level behaviour. Such a description is necesssary, for example, when one needs to take into account the excluded volume effects or steric shielding [14]. Cellular cytoplasm and cell membranes are crowded with proteins and lipids, and the molecular crowding is difficult to model if macromolecules are approximated as points [8]. Although we did not include the excluded volume interactions in this paper, the two-parameter λ-$\bar{\varrho}$ model is more suitable to address these problems than the one-parameter models studied in Section 3.2, simply because we can separate the length of interaction ($\bar{\varrho}$) from its probability (P_λ). Obviously, there is a possibility to design molecular-based models with more than two parameters. For example, one could simulate the bimolecular reaction $A + B \rightarrow C$ by specifying the probability $P(r, \Delta t)$ that a molecule of A and a molecule of B, which are the distance r apart, react in the next time step. In this case, $P(r, \Delta t)$ is a function which can have as many degrees of freedom as we want and could further depend on the rotation of molecules. The λ-$\bar{\varrho}$ model is a special case of this framework provided that we choose $P(r, \Delta t) = P_\lambda$ for $r \leq \bar{\varrho}$ and otherwise zero. Considering $P(r, \Delta t)$ with more degrees of freedom, there is the potential to include more molecular-level biophysics which can be precomputed by detailed Brownian dynamics simulations [30]. However, this would go beyond the scope of this manuscript. Another advantage of the λ-$\bar{\varrho}$ model is that it can be used to understand connections between

the molecular-based and the compartment-based approaches. In both the λ-$\bar{\varrho}$ and the compartment-based models, a molecule of A reacts with the given rate whenever it is in the neighborhood of a molecule of B. Here, the neighborhood is either a ball or a cube, depending on the model. The λ-$\bar{\varrho}$ model can be thought as a generalization of the particle-based models from Section 3.2 which makes them directly comparable to the compartment-based models from Section 3.1 - see also discussion in Section 5 for more details. This sheds more light on the problem of equivalence of on-lattice and off-lattice stochastic modelling of reaction-diffusion processes [26].

5. Discussion

In this paper, we used the illustrative examples (1) and (5) to compare the results of different stochastic reaction-diffusion methods. The advantage of illustrative chemical models (1) and (5) is that they have non-trivial stationary distributions given by (3) and (7), respectively. In principle, one could study $A + B \rightarrow B$ (or $A + A \rightarrow B$) on its own to make the illustrative examples even simpler. However, the number of molecules of A would then decrease to zero as time progresses and the stationary distribution would be trivial (i.e. there would be 0 molecules with probability 1 in the system after long time). The trivial stationary distribution is obtained for $A + B \rightarrow B$ (or $A + A \rightarrow B$) by any reaction-diffusion SSA, so we would not learn anything useful from the stationary behaviour. We would observe differences in modelling the transient behaviour of bimolecular reactions. However, the transient behaviour depends on the initial condition. For these reasons, we coupled bimolecular reactions with the production of the chemical species A to obtain the model chemical systems (1) and (5) which have the non-trivial stationary distributions. It is worth noting that the model systems in this paper do not have any spatial variation of the probability distribution. No part of the computational domain is preferred by molecules of A or B and the resulting probability distribution is homogeneous in space. It is easy to generalize (1) and (5) to the spatially non-homogeneous case (for example, by considering production reaction $\emptyset \rightarrow A$ only in part of the computational domain [16]). Such a generalization is necessary for studying some other aspects of reaction-diffusion SSAs which we will address in a future publication. However, our examples (1) and (5) were complex enough to illustrate all results of this paper.

We studied both on-lattice and off-lattice SSAs for reaction-diffusion processes. In particular, we were able to see connections between both types of models. For on-lattice models we found that there was a limitation on the compartment size h from below, i.e. $h \geq h_{crit}$. In Section 4.1, we showed that the rate of bimolecular reaction per compartment must be chosen to be infinity for $h = h_{crit}$. In a similar way for the off-lattice model, a decrease of $\bar{\varrho}$ in the λ-$\bar{\varrho}$ model, presented in Section 3.2, must be compensated by an increase in the rate λ (probability P_λ). Again, there is a limitation on $\bar{\varrho}$ from below, i.e. $\bar{\varrho}$ must be larger than or equal to the ϱ of the Smoluchowski model which is given by (21). If $\bar{\varrho}$ is sufficiently larger than this limiting value, then λ is given

by (32), that is, the reaction rate constant k_1 divided by the volume, $4\pi\overline{\varrho}^3/3$, of the ball in which the reaction takes place. This is analogous to the situation $h \gg h_{crit}$ where the reaction rate per compartment is given by k_1/h^3 (reaction rate constant k_1 divided by the volume, h^3, of the compartment). Thus both models give, in the limit of large $\overline{\varrho}$ and large h, the same expression for local reaction rates: the rate constant divided by the volume in which the reaction takes place.

The examples studied in this paper contained only irreversible bimolecular reactions. However, it is worth noting that the idea of the λ-$\overline{\varrho}$ model can also resolve the problem of the "geminate recombination" associated with some molecular-based approaches to modelling reversible reactions [3, 2]. This problem can be described as follows. Consider the reversible bimolecular reaction $A + B \rightleftarrows C$. It consists of two reactions: the bimolecular reaction $A + B \rightarrow C$ and the reverse reaction $C \rightarrow A + B$ which is of first-order. When the complex C dissociates according to the reverse reaction $C \rightarrow A + B$, one has to specify the initial positions of new molecules of A and B which are created. The most natural choice is to put new molecules of A and B at the position of the complex C before the reaction occurred. However, the new molecules might immediately react again according to the forward reaction. Andrews and Bray [3] solve this problem by introducing the so called unbinding radius (i.e. a finite initial separation of the molecules A and B). This artificial concept is not needed in the λ-$\overline{\varrho}$ model provided that P_λ is small (i.e. $P_\lambda \ll 1$) which is often the case. If the new molecules are placed close to each other (at the position of C), they have only a small probability of reacting and can diffuse away of each other. We have to be more careful for larger values of the probability P_λ because the algorithm is, in the limit $P_\lambda \rightarrow 1$, equivalent to the Andrews and Bray algorithm [3]. If P_λ is close to one, then their concept of the unbinding radius offers a possible solution to the problem of "geminate recombination". We are currently investigating the behaviour of stochastic reaction-diffusion algorithms for systems with reversible reactions and will report our findings in a future publication.

The results of this paper have been summarized in Section 4. They were explained on illustrative computational examples, but the general formulae can be applied to modelling bimolecular reactions which are part of complex reaction-diffusion processes. We presented our results as improvements of two commonly used reaction-diffusion SSAs which have been previously implemented in reaction-diffusion software packages MesoRD [24] and Smoldyn [3]. Other molecular-based models, such as MCell [34], Green's-function reaction dynamics [39, 36] and velocity jump processes [13, 17], were not directly studied in this paper but some of the ideas presented in Section 4.2 can be applied to improve them too. From the application point of view, we focussed on modelling bimolecular reactions of biomolecules, e.g. proteins, but the concepts presented can be also applied to stochastic reaction-diffusion modelling in population ecology [28] or to modelling cellular dispersal [18, 19]. In these cases, the diffusing objects are not macromolecules but cells or animals, and the bimolecular "reaction" is not a chemical reaction but local interaction between two cells or animals, for example,

competition or predation [28].

Glossary

Gillespie SSA. Stochastic simulation algorithm for simulating the time-evolution of well-stirred chemical systems. The results are consistent with the solution of the chemical master equation [21, 22].

Markov Chain. Stochastic process for which the future states of the system only depend on the present state and are independent of the past states.

Modified Bessel function of the first kind. The evaluation of modified Bessel functions is part of any standard mathematical software (e.g. the function `besseli` in Matlab). In general, the modified Bessel function I_n (for $n \in \mathbb{N}$) is a solution of the ordinary differential equation

$$z^2 \, I_n''(z) + z \, I_n'(z) - (z^2 + n^2) \, I_n(z) = 0.$$

Acknowledgments

Appendix A. Stationary distributions, means and variances for the illustrative heteroreaction and homoreaction examples

Let us consider chemical system (1) to be well-stirred. Let $p_n(t)$ be the probability that there are n molecules of A at time t in the reactor, i.e. $A(t) = n$. Then $p_n(t)$ evolves according to the chemical master equation [16, 23]

$$\frac{\mathrm{d}p_n}{\mathrm{d}t} = \frac{k_1 B_0}{\nu} \, (n+1) \, p_{n+1} - \frac{k_1 B_0}{\nu} \, n \, p_n + k_2 \nu \, p_{n-1} - k_2 \nu \, p_n \qquad \text{(A.1)}$$

where the third term on the right hand side is missing in (A.1) for $n = 0$; i.e. we use the convention that $p_{-1} \equiv 0$. The stationary distribution $\phi(n)$ is defined by

$$\phi(n) = \lim_{t \to \infty} p_n(t). \qquad \text{(A.2)}$$

Consequently, (A.1) implies that $\phi(n)$ satisfies the equation

$$\frac{k_1 B_0}{\nu} \, (n+1) \, \phi(n+1) - \frac{k_1 B_0}{\nu} n \, \phi(n) + k_2 \nu \, \phi(n-1) - k_2 \nu \, \phi(n) = 0$$

where $\phi(-1) = 0$, which can be equivalently written as

$$\phi(1) = \frac{k_2 \nu^2}{k_1 B_0} \, \phi(0),$$

$$\phi(n) = \left(\frac{k_2 \nu^2}{k_1 B_0 n} + 1 - \frac{1}{n} \right) \phi(n-1) - \frac{k_2 \nu^2}{k_1 B_0 n} \, \phi(n-2), \quad \text{for } n \geq 2. \quad \text{(A.3)}$$

Thus $\phi(n)$ is uniquely determined by the value of $\phi(0)$. We can easily verify that (3) satisfies (A.3). Moreover, it is the only solution of (A.3) that satisfies the normalization condition $\sum_{n=0}^{\infty} \phi(n) = 1$. The stationary value of the stochastic mean M_s (i.e. the value around which the number of molecules fluctuates) and the stationary value of the variance V_s (i.e. the size of the stochastic fluctuations) are given by

$$M_s = \sum_{n=0}^{\infty} n\,\phi(n), \qquad V_s = \sum_{n=0}^{\infty} (n - M_s)^2\,\phi(n). \tag{A.4}$$

Using (3), we obtain (4) and $V_s = M_s$.

Let us consider the homoreaction example (5). Then the chemical master equation reads as follows

$$\frac{\mathrm{d}p_n}{\mathrm{d}t} = \frac{k_1}{\nu}\,(n+2)(n+1)\,p_{n+2} - \frac{k_1}{\nu}\,n(n-1)\,p_n + k_2\nu\,p_{n-1} - k_2\nu\,p_n.$$

Starting with the stationary version of this equation, one can use the method of moment generating function [38] to show that the stationary distribution $\phi(n)$ is given by (7) [11, 37]. The stationary values of stochastic mean M_s and variance V_s, which are defined by (A.4), can be also evaluated in terms of the Bessel functions; M_s is given by (8) and $V_s = M_s - M_s^2 + k_2\nu^2/(2k_1)$. The classical deterministic description of the chemical system (5) is given, for concentration $a(t) = A(t)/\nu$, as the ODE $\mathrm{d}a/\mathrm{d}t = -2k_1 a^2 + k_2$. Multiplying by ν, we obtain the ODE

$$\frac{\mathrm{d}\overline{A}}{\mathrm{d}t} = -\frac{2k_1}{\nu}\,\overline{A}^2 + k_2\nu \tag{A.5}$$

where $\overline{A}(t) = a(t)\nu$ is the deterministic approximation of the average number of molecules in the volume ν with concentration $a(t)$. Notice that equation (A.5) does not give us the time evolution of the stochastic mean. To see that, let us consider the stationary value of $\overline{A}(t)$. It is given as the solution of the stationary equation corresponding to (A.5), namely $0 = -2k_1/\nu\overline{A}_s^2 + k_2\nu$. Hence, $\overline{A}_s = \nu\sqrt{k_2/(2k_1)}$ which is not equal to M_s given by formula (8). See also the discussion at the end of Section 2.2.

Appendix B. Reaction-diffusion master equation

Let $\mathbb{N} = \{0, 1, 2, 3, \ldots\}$ be the set of non-negative integers. Let $\mathbf{n} \in \mathbb{N}^{I_{all}}$ and $\mathbf{m} \in \mathbb{N}^{I_{all}}$. We denote their coordinates by three indices, namely

$$\mathbf{n} = \{n_{ijk} \,|\, (i, j, k) \in I_{all}\} \qquad \text{and} \qquad \mathbf{m} = \{m_{ijk} \,|\, (i, j, k) \in I_{all}\}. \tag{B.1}$$

Let $p(\mathbf{n}, \mathbf{m}, t)$ be the joint probability that $A_{ijk}(t) = n_{ijk}$ and $B_{ijk}(t) = m_{ijk}$ for all $(i, j, k) \in I_{all}$. The reaction-diffusion master equation describes the time evolution of $p(\mathbf{n}, \mathbf{m}, t)$. To formulate it, we define the operators $J_{ijk}^{\mathbf{e}} : \mathbb{N}^{I_{all}} \to \mathbb{N}^{I_{all}}$ for $(i, j, k) \in I_{all}$ and $\mathbf{e} \in \mathbf{E}_{ijk}$ by

$$J_{ijk}^{\mathbf{e}}(\mathbf{n}) = \{q_{uvw} \,|\, (u, v, w) \in I_{all}\}$$

where

$$q_{uvw} = \begin{cases} n_{uvw} + 1, & \text{for } (u, v, w) = (i, j, k); \\ n_{uvw} - 1, & \text{for } (u, v, w) = (i, j, k) + \mathbf{e}; \\ n_{uvw}, & \text{otherwise.} \end{cases}$$

We also define

$$\boldsymbol{\delta}_{ijk} = \{\delta_{uvw} \,|\, (u, v, w) \in I_{all}\} \quad \text{where} \quad \delta_{uvw} = \begin{cases} 1, & \text{for } (u, v, w) = (i, j, k); \\ 0, & \text{otherwise.} \end{cases}$$

Then the reaction-diffusion master equation, i.e. the chemical master equation which corresponds to the system of "chemical reactions" (9)–(11), can be written as follows [22, 23]

$$\begin{aligned}
\frac{\partial p(\mathbf{n}, \mathbf{m})}{\partial t} &= \frac{k_1}{h^3} \sum_{(i,j,k) \in I_{all}} \left\{ (n_{ijk} + 1) m_{ijk}\, p(\mathbf{n} + \boldsymbol{\delta}_{ijk}, \mathbf{m}) - n_{ijk} m_{ijk}\, p(\mathbf{n}, \mathbf{m}) \right\} \\
&\quad + k_2 h^3 \sum_{(i,j,k) \in I_{all}} \left\{ p(\mathbf{n} - \boldsymbol{\delta}_{ijk}, \mathbf{m}) - p(\mathbf{n}, \mathbf{m}) \right\} \qquad\qquad\text{(B.2)} \\
&\quad + \frac{D_A}{h^2} \sum_{(i,j,k) \in I_{all}} \sum_{\mathbf{e} \in \mathbf{E}_{ijk}} \left\{ (n_{ijk} + 1)\, p(J^{\mathbf{e}}_{ijk}(\mathbf{n}), \mathbf{m}) - n_{ijk}\, p(\mathbf{n}, \mathbf{m}) \right\} \\
&\quad + \frac{D_B}{h^2} \sum_{(i,j,k) \in I_{all}} \sum_{\mathbf{e} \in \mathbf{E}_{ijk}} \left\{ (m_{ijk} + 1)\, p(\mathbf{n}, J^{\mathbf{e}}_{ijk}(\mathbf{m})) - m_{ijk}\, p(\mathbf{n}, \mathbf{m}) \right\}.
\end{aligned}$$

The first two terms on the right hand side correspond to chemical reactions (9), the third term to diffusion jumps (10) and the last term to diffusion jumps (11).

Appendix C. Derivation of formulae (26) and (27)

We will first study the case $D_B = 0$ and $B_0 = 1$. This means that there is only one molecule of B in the system and it does not diffuse. In particular, reactions (11) are not included in the model. Let the molecule of B be in the compartment $\bar{b} = (b_1, b_2, b_3) \in I_{all}$. Let $\mathbf{n} \in \mathbb{N}^{I_{all}}$ with the coordinates defined by (B.1). Let $p(\mathbf{n}, t)$ be the joint probability that $A_{ijk}(t) = n_{ijk}$ for all $(i, j, k) \in I_{all}$. Since the position of the molecule of B does not evolve, the reaction-diffusion master equation (B.2) simplifies to the following equation for $p(\mathbf{n}, t)$

$$\begin{aligned}
\frac{\partial p(\mathbf{n})}{\partial t} &= \frac{k_1}{h^3} \left\{ (n_{\bar{b}} + 1)\, p(\mathbf{n} + \boldsymbol{\delta}_{\bar{b}}) - n_{\bar{b}}\, p(\mathbf{n}) \right\} + k_2 h^3 \sum_{(i,j,k) \in I_{all}} \left\{ p(\mathbf{n} - \boldsymbol{\delta}_{ijk}) - p(\mathbf{n}) \right\} \\
&\quad + \frac{D_A}{h^2} \sum_{(i,j,k) \in I_{all}} \sum_{\mathbf{e} \in \mathbf{E}_{ijk}} \left\{ (n_{ijk} + 1)\, p(J^{\mathbf{e}}_{ijk}(\mathbf{n})) - n_{ijk}\, p(\mathbf{n}) \right\}. \qquad\text{(C.1)}
\end{aligned}$$

We want to change the reaction rate k_1/h^3 (of the bimolecular reaction per one compartment) to a reaction rate λ in order to decrease the error between stationary

distributions ϕ_K and ϕ_1. The stationary version of (C.1) with k_1/h^3 replaced by λ is

$$\lambda\Big\{(n_{\overline{b}}+1)\,p_s(\mathbf{n}+\boldsymbol{\delta}_{\overline{b}}) - n_{\overline{b}}\,p_s(\mathbf{n})\Big\} + k_2 h^3 \sum_{(i,j,k)\in I_{all}} \Big\{p_s(\mathbf{n}-\boldsymbol{\delta}_{ijk}) - p_s(\mathbf{n})\Big\}$$

$$+\; \frac{D_A}{h^2}\sum_{(i,j,k)\in I_{all}}\sum_{\mathbf{e}\in\mathbf{E}_{ijk}}\Big\{(n_{ijk}+1)\,p_s(J_{ijk}^{\mathbf{e}}(\mathbf{n})) - n_{ijk}\,p_s(\mathbf{n})\Big\} \;=\; 0 \qquad \text{(C.2)}$$

where

$$p_s(\mathbf{n}) = \lim_{t\to\infty} p(\mathbf{n},t). \tag{C.3}$$

Let us denote the average number of molecules at the lattice site (i,j,k) as

$$M_{ijk}(t) = \sum_{\mathbf{n}} n_{ijk}\, p_s(\mathbf{n}) \equiv \sum_{n_{111}=0}^{\infty}\sum_{n_{112}=0}^{\infty}\cdots\sum_{n_{KKK}=0}^{\infty} n_{ijk}\, p_s(\mathbf{n}).$$

Multiplying (C.2) by n_{ijk} and summing over $\mathbf{n}$, we obtain

$$k_2 h^3 + \frac{D_A}{h^2}\sum_{\mathbf{e}\in\mathbf{E}_{ijk}}(M_{ijk+\mathbf{e}} - M_{ijk}) = 0, \qquad \text{for } (i,j,k)\neq\overline{b}, \tag{C.4}$$

$$k_2 h^3 + \frac{D_A}{h^2}\sum_{\mathbf{e}\in\mathbf{E}_{\overline{b}}}(M_{\overline{b}+\mathbf{e}} - M_{\overline{b}}) \qquad = \lambda M_{\overline{b}}. \tag{C.5}$$

Let us define tensors $\psi^{i'j'k'}\in\mathbb{R}^{K\times K\times K}$, for $i'=0,1,2,\ldots,K-1$; $j'=0,1,2,\ldots,K-1$ and $k'=0,1,2,\ldots,K-1$, by

$$\psi_{ijk}^{i'j'k'} = \frac{1}{K^{3/2}}\,\cos\left(\frac{i'(i-1/2)\pi}{K}\right)\times\cos\left(\frac{j'(j-1/2)\pi}{K}\right)\times\cos\left(\frac{k'(k-1/2)\pi}{K}\right)$$

$$\times\;\begin{cases}\sqrt{8}, & \text{if } i',\,j',\,k' \text{ are nonzero;}\\ \sqrt{4}, & \text{if exactly one of } i',\,j',\,k' \text{ is zero;}\\ \sqrt{2}, & \text{if exactly two of } i',\,j',\,k' \text{ are zero;}\\ 1, & \text{for } i'=j'=k'=0.\end{cases} \tag{C.6}$$

We have

$$\sum_{i=1}^{K}\cos\left(\frac{i'(i-1/2)\pi}{K}\right)\cos\left(\frac{i''(i-1/2)\pi}{K}\right) = \delta_{i'i''}\frac{K}{2}, \qquad \text{for } i'>0,$$

where $\delta_{i'i''}$ is the Kronecker delta. Consequently, $\psi^{i'j'k'}$, for $i',j',k'=0,1,\ldots,K-1$, satisfy the orthonormality condition:

$$\sum_{i,j,k=1}^{K}\psi_{ijk}^{i'j'k'}\psi_{ijk}^{i''j''k''} = \delta_{i'i''}\delta_{j'j''}\delta_{k'k''}. \tag{C.7}$$

Let us express M_{ijk} in the basis $\psi^{i'j'k'}$:

$$M_{ijk} = \sum_{i',j',k'=0}^{K-1} \widetilde{M}_{i'j'k'}\,\psi_{ijk}^{i'j'k'}. \tag{C.8}$$

Then (C.4)–(C.5) read as follows

$$k_2 h^3 + \frac{D_A}{h^2} \sum_{i',j',k'=0}^{K-1} \widetilde{M}_{i'j'k'} \sum_{\mathbf{e} \in \mathbf{E}_{ijk}} \left(\psi_{ijk+\mathbf{e}}^{i'j'k'} - \psi_{ijk}^{i'j'k'} \right) = 0, \quad \text{for } (i,j,k) \neq \bar{b},$$

$$k_2 h^3 + \frac{D_A}{h^2} \sum_{i',j',k'=0}^{K-1} \widetilde{M}_{i'j'k'} \sum_{\mathbf{e} \in \mathbf{E}_{\bar{b}}} \left(\psi_{\bar{b}+\mathbf{e}}^{i'j'k'} - \psi_{\bar{b}}^{i'j'k'} \right) = \lambda M_{\bar{b}}.$$

Using (C.6), we get

$$k_2 h^3 + \frac{D_A}{h^2} \sum_{i',j',k'=0}^{K-1} \widetilde{M}_{i'j'k'} \, c^{i'j'k'} \, \psi_{ijk}^{i'j'k'} = 0, \quad \text{for } (i,j,k) \neq \bar{b}, \tag{C.9}$$

$$k_2 h^3 + \frac{D_A}{h^2} \sum_{i',j',k'=0}^{K-1} \widetilde{M}_{i'j'k'} \, c^{i'j'k'} \, \psi_{\bar{b}}^{i'j'k'} = \lambda M_{\bar{b}}, \tag{C.10}$$

where

$$c^{ijk} = 2 \left(\cos\left(\frac{i\pi}{K}\right) + \cos\left(\frac{j\pi}{K}\right) + \cos\left(\frac{k\pi}{K}\right) - 3 \right). \tag{C.11}$$

Multiplying (C.9)–(C.10) by $\psi_{ijk}^{i''j''k''}$, summing the resulting equations and using the orthonormality condition (C.7), we obtain

$$k_2 \nu = \lambda M_{\bar{b}}, \tag{C.12}$$

$$\frac{D_A}{h^2} c^{i''j''k''} \widetilde{M}_{i''j''k''} = \lambda M_{\bar{b}} \psi_{\bar{b}}^{i''j''k''}, \qquad \text{for } (i'', j'', k'') \neq (0,0,0),$$

where $\nu = L^3 = h^3 K^3$ is the volume of the reactor. We drop the double primes on indices i, j and k to simplify the notation and obtain

$$\widetilde{M}_{ijk} = \frac{\lambda \, h^2 M_{\bar{b}} \, \psi_{\bar{b}}^{ijk}}{D_A \, c^{ijk}}, \qquad \text{for } (i,j,k) \neq (0,0,0).$$

Using (C.12), we get

$$\widetilde{M}_{ijk} = \frac{k_2 \nu \, h^2 \, \psi_{\bar{b}}^{ijk}}{D_A \, c^{ijk}}, \qquad \text{for } (i,j,k) \neq (0,0,0). \tag{C.13}$$

Using (C.8) and (C.13), we have

$$M_{\bar{b}} = \sum_{i,j,k=0}^{K-1} \widetilde{M}_{ijk} \, \psi_{\bar{b}}^{ijk} = K^{-3/2} \widetilde{M}_{000} - \frac{k_2 \nu \, h^2}{D_A} \beta_{\bar{b}} \tag{C.14}$$

where

$$\beta_{\bar{b}} = - \sum_{\substack{i,j,k=0 \\ (i,j,k) \neq (0,0,0)}}^{K-1} \frac{(\psi_{\bar{b}}^{ijk})^2}{c^{ijk}}. \tag{C.15}$$

Substituting (C.12) into (C.14), we have

$$\frac{k_2 \nu}{\lambda} = K^{-3/2} \widetilde{M}_{000} - \beta_{\bar{b}} \frac{k_2 \nu \, h^2}{D_A}. \tag{C.16}$$

The average number of molecules of A in the reactor is given by

$$A_s \equiv \sum_{i,j,k=1}^{K} M_{ijk}.$$

Using (C.8), we get

$$A_s = \sum_{i,j,k=1}^{K} \sum_{i',j',k'=0}^{K-1} \widetilde{M}_{i'j'k'} \, \psi_{ijk}^{i'j'k'} = \sum_{i',j',k'=0}^{K-1} \widetilde{M}_{i'j'k'} \sum_{i,j,k=1}^{K} \psi_{ijk}^{i'j'k'} = \widetilde{M}_{000} \, K^{3/2}. \qquad \text{(C.17)}$$

We would like to choose λ so that $A_s = M_s$ where M_s is given by (4), i.e.

$$\frac{k_2 \nu^2}{k_1} = \widetilde{M}_{000} \, K^{3/2}.$$

Substituting for $\widetilde{M}_{000}$ into (C.16) and using $\nu = h^3 K^3$, we get

$$\frac{k_2 \nu}{\lambda} = h^3 \frac{k_2 \nu}{k_1} - \beta_{\bar{b}} \frac{k_2 \nu \, h^2}{D_A}$$

which implies

$$\lambda = \frac{D_A k_1}{D_A h^3 - \beta_{\bar{b}} \, k_1 h^2}.$$

This choice of λ gives the average number of molecules of A equal to M_s, provided that $D_B = 0$, $B_0 = 1$ and the molecule of B is in the compartment $\bar{b} = (b_1, b_2, b_3) \in I_{all}$.

Now let $D_B \neq 0$ and $B_0 = 1$. If we want to model the bimolecular reaction (1), it is important to know the distances of molecules of A from the molecule of B. The distances diffuse with the diffusion constant $D_A + D_B$. Thus we can equivalently model their time evolution by considering that the molecule of B does not diffuse and molecules of A diffuse with the diffusion constant $D_A + D_B$. Then the previous calculation (equation (C.16)) implies that

$$K^{-3/2} \widetilde{M}_{000}^{\bar{b}} = \frac{k_2 \nu}{\lambda} + \beta_{\bar{b}} \frac{k_2 \nu \, h^2}{D_A + D_B} \qquad \text{(C.18)}$$

where notation $\widetilde{M}_{000}^{\bar{b}} \equiv \widetilde{M}_{000}$ highlights the fact that $\widetilde{M}_{000}$ depends on the position $\bar{b}$ of the molecule of B. Let $p_{\bar{b}}$ be the probability that the molecule of B is in the compartment $\bar{b} = (b_1, b_2, b_3) \in I_{all}$. We have $p_{\bar{b}} = K^{-3}$. The average number of molecules of A in the reactor is given by (compare with (C.17))

$$A_s \equiv \sum_{\bar{b}} p_{\bar{b}} \widetilde{M}_{000}^{\bar{b}} \, K^{3/2} = K^{-3/2} \sum_{\bar{b}} \widetilde{M}_{000}^{\bar{b}}.$$

Multyplying (C.18) by $p_{\bar{b}} = K^{-3}$ and summing over $\bar{b}$, we obtain

$$\frac{A_s}{K^3} = \frac{k_2 \nu}{\lambda} + \beta \frac{k_2 \nu \, h^2}{D_A + D_B} \qquad \text{(C.19)}$$

where

$$\beta = \sum_{\bar{b}} p_\beta \, \beta_{\bar{b}} = \frac{1}{K^3} \sum_{\bar{b}} \beta_{\bar{b}}. \qquad \text{(C.20)}$$

We would like to choose λ so that $A_s = M_s$ where M_s is given by (4). Substituting (4) into (C.19), we get

$$\frac{k_2 \nu^2}{k_1 K^3} = \frac{k_2 \nu}{\lambda} + \beta \frac{k_2 \nu h^2}{D_A + D_B}.$$

Using $\nu = h^3 K^3$, we obtain

$$\lambda = \frac{(D_A + D_B)k_1}{(D_A + D_B)h^3 - \beta k_1 h^2}.$$

Thus we have derived (26). Using (C.20), (C.15) and orthonormality condition (C.7), we obtain

$$\beta = \frac{1}{K^3} \sum_{\bar{b}} \beta_{\bar{b}} = -\frac{1}{K^3} \sum_{\substack{i,j,k=0 \\ (i,j,k) \neq (0,0,0)}}^{K-1} \sum_{\bar{b}} \frac{(\psi_{\bar{b}}^{ijk})^2}{c^{ijk}} = -\frac{1}{K^3} \sum_{\substack{i,j,k=0 \\ (i,j,k) \neq (0,0,0)}}^{K-1} \frac{1}{c^{ijk}}.$$

Substituting (C.11) for c^{ijk}, we obtain (27).

Appendix D. Derivation of formula (28)

Formula (27) is the Riemann sum of the definite integral

$$\beta_\infty = \frac{1}{2(\pi)^3} \int_0^\pi \int_0^\pi \int_0^\pi \frac{1}{3 - \cos x - \cos y - \cos z} \, \mathrm{d}x \, \mathrm{d}y \, \mathrm{d}z, \qquad (\text{D.1})$$

i.e., passing $K \to \infty$ in (27), we obtain (D.1). Integrating over z, we get (28).

Formula (28) can be also derived directly without the help of (27). Such a derivation uses a similar reasoning as the derivation of (31) in Appendix E, i.e. it establishes a link between molecular-based models and the compartment-based modelling. We consider the infinite three-dimensional lattice

$$(i, j, k)h \qquad \text{for } i \in \mathbb{Z},\ j \in \mathbb{Z},\ k \in \mathbb{Z} \qquad (\text{D.2})$$

where $h \in \mathbb{R}$. To model bimolecular reactions by the compartment-based approach, we need to know whether the molecules are in the same compartment or not. In particular, it is sufficient to track the relative distance of molecules rather than their absolute positions. Postulating that the molecule of B is always at the origin (compartment $(0,0,0)$) and letting the molecule of A diffuse with the diffusion constant $(D_A + D_B)$, we obtain the stochastic model which gives the same distribution of relative distances of molecules as the original stochastic model. Thus we will study the following auxiliary stochastic process. We consider that the particles jump to neighbouring lattice sites with the rate $(D_A + D_B)/h^2$ and are removed at the origin with the rate λ. The reaction-diffusion master equation can be written for this model as follows (using the same notation as in (B.2))

$$\frac{\partial p(\mathbf{n})}{\partial t} = \frac{D_A + D_B}{h^2} \sum_{(i,j,k) \in \mathbb{Z}^3} \sum_{\mathbf{e} \in \mathbf{E}} \left\{ (n_{ijk} + 1)\, p(J_{ijk}^{\mathbf{e}}(\mathbf{n})) - n_{ijk}\, p(\mathbf{n}) \right\}$$

$$+ \lambda \left\{ (n_{000} + 1)\, p(\mathbf{n} + \boldsymbol{\delta}_{000}) - n_{000}\, p(\mathbf{n}) \right\}. \qquad (\text{D.3})$$

We are interested in the stationary behaviour of a system of (infinitely) many molecules of A, subject to the condition that the average number of molecules per compartment is kept constant (equal to M_∞) far from the origin, i.e. in the limit $\sqrt{i^2 + j^2 + k^2} \to \infty$. The stationary version of (D.3) reads as follows

$$\frac{D_A + D_B}{h^2} \sum_{(i,j,k) \in \mathbb{Z}^3} \sum_{\mathbf{e} \in \mathbf{E}} \left\{ (n_{ijk} + 1) \, p_s(J_{ijk}^{\mathbf{e}}(\mathbf{n})) - n_{ijk} \, p_s(\mathbf{n}) \right\}$$

$$= -\lambda \left\{ (n_{000} + 1) \, p_s(\mathbf{n} + \boldsymbol{\delta}_{000}) - n_{000} \, p_s(\mathbf{n}) \right\} \tag{D.4}$$

where $p_s(\mathbf{n})$ is defined as in (C.3). Let us denote the average number of molecules at the lattice site (i, j, k) as

$$M_{ijk}(t) = \sum_{\mathbf{n}} n_{ijk} p_s(\mathbf{n}).$$

Multiplying (D.4) by n_{ijk} and summing over $\mathbf{n}$, we obtain

$$\frac{D_A + D_B}{h^2} \sum_{\mathbf{e} \in \mathbf{E}} (M_{ijk+\mathbf{e}} - M_{ijk}) = 0 \qquad \text{for } (i, j, k) \neq (0, 0, 0),$$

$$\frac{D_A + D_B}{h^2} \sum_{\mathbf{e} \in \mathbf{E}} (M_{\mathbf{e}} - M_{000}) \quad = \lambda M_{000}.$$

Let us define $\mu_{ijk} = M_{ijk} - M_\infty$. Then we have

$$\sum_{\mathbf{e} \in \mathbf{E}} \mu_{ijk+\mathbf{e}} = 6\mu_{ijk}, \qquad \text{for } (i, j, k) \neq (0, 0, 0),$$

$$\sum_{\mathbf{e} \in \mathbf{E}} \mu_{\mathbf{e}} \quad = 6\mu_{000} + \frac{\lambda h^2}{D_A + D_B} \left(\mu_{000} + M_\infty \right).$$

Multiplying by $e^{\mathbf{i} x i} e^{\mathbf{i} y j} e^{\mathbf{i} z k}$, where $\mathbf{i} = \sqrt{-1}$, $x \in \mathbb{R}$, $y \in \mathbb{R}$, $z \in \mathbb{R}$, and summing over i, j and k, we obtain

$$6 \, \widehat{\mu}_{xyz} = \widehat{\mu}_{xyz} \left(e^{\mathbf{i} x} + e^{-\mathbf{i} x} + e^{\mathbf{i} y} + e^{-\mathbf{i} y} + e^{\mathbf{i} z} + e^{-\mathbf{i} z} \right)$$
$$- \lambda h^2 \left(\mu_{000} + M_\infty \right) / (D_A + D_B) \tag{D.5}$$

where $\widehat{\mu}_{xyz}$ is the Fourier transform

$$\widehat{\mu}_{xyz} = \sum_{i=-\infty}^{\infty} \sum_{j=-\infty}^{\infty} \sum_{k=-\infty}^{\infty} e^{\mathbf{i} x i} e^{\mathbf{i} y j} e^{\mathbf{i} z k} \mu_{ijk}.$$

Simplifying (D.5), we obtain

$$\widehat{\mu}_{xyz} = \frac{\lambda h^2 \left(\mu_{000} + M_\infty \right)}{2(D_A + D_B)} \frac{1}{\cos x + \cos y + \cos z - 3}.$$

Thus

$$\mu_{000} = -\beta_\infty \frac{\lambda h^2 \left(\mu_{000} + M_\infty \right)}{D_A + D_B} \tag{D.6}$$

where β_∞ is the constant given by

$$\beta_\infty = \frac{1}{2(2\pi)^3} \int_0^{2\pi} \int_0^{2\pi} \int_0^{2\pi} \frac{1}{3 - \cos x - \cos y - \cos z} \, \mathrm{d}x \, \mathrm{d}y \, \mathrm{d}z. \tag{D.7}$$

Using $\mu_{000} = M_{000} - M_\infty$, equation (D.6) can be rewritten as

$$\lambda M_{000} = \frac{\lambda (D_A + D_B)}{(D_A + D_B) + \lambda \beta_\infty h^2} M_\infty. \tag{D.8}$$

The term λM_{000} gives the rate of removal of molecules of A at the origin. The rate of change of the concentration a of molecules of A, which is subject to heteroreaction (1), can be also described by the deterministic ODE $da/dt = -k_1 ab$ where b is the concentration of molecules of B. This ODE can be equivalently rewritten in terms of the average numbers of molecules of A and B per lattice site, i.e. in terms of $A = ah^3$ and $B = bh^3$, as $dA/dt = -k_1/h^3 AB$. Using $B = 1$ and $A = M_\infty$, the rate of removal of molecules of A is given by $k_1/h^3 M_\infty$. Comparing with (D.8), we obtain

$$\frac{k_1}{h^3} M_\infty = \frac{\lambda (D_A + D_B)}{(D_A + D_B) + \lambda \beta_\infty h^2} M_\infty.$$

Solving for λ, we obtain

$$\lambda = \frac{(D_A + D_B)k_1}{(D_A + D_B)h^3 - \beta_\infty k_1 h^2}.$$

Thus we have derived (26) with $\beta = \beta_\infty$. The constant β_∞ is given by (D.7). Using periodicity of the cosine function, we obtain (D.1). Integrating over z, we derive (28).

Appendix E. Derivation of formula (31)

In order to derive (31), we consider the diffusion to the ball of radius $\bar{\varrho}$ which removes molecules of A with the rate λ. Let the centre of the ball be at the origin. Let $c(r)$ be the equilibrium concentration of molecules of A at distance r from the origin, which is a continuous function with continuous derivative satisfying the equations

$$\frac{\mathrm{d}^2 c}{\mathrm{d}r^2} + \frac{2}{r}\frac{\mathrm{d}c}{\mathrm{d}r} = 0, \qquad \text{for } r \geq \bar{\varrho},$$

$$\frac{\mathrm{d}^2 c}{\mathrm{d}r^2} + \frac{2}{r}\frac{\mathrm{d}c}{\mathrm{d}r} - \frac{\lambda c}{D_A + D_B} = 0, \qquad \text{for } r \leq \bar{\varrho}.$$

The general solution of these second-order ODEs can be written in the following form

$$c(r) = a_1 + \frac{a_2}{r}, \qquad \text{for } r \geq \bar{\varrho},$$

$$c(r) = \frac{a_3}{r} \exp\left[r\sqrt{\frac{\lambda}{D_A + D_B}}\right] + \frac{a_4}{r} \exp\left[-r\sqrt{\frac{\lambda}{D_A + D_B}}\right], \qquad \text{for } r \leq \bar{\varrho},$$

where a_1, a_2, a_3 and a_4 are real constants. We impose the boundary condition at infinity

$$\lim_{r \to \infty} c(r) = c_\infty.$$

This implies $a_1 = c_\infty$. Since c is continuous at the origin, we deduce $a_4 = -a_3$. Thus we have

$$c(r) = c_\infty + \frac{a_2}{r}, \qquad \text{for } r \geq \bar{\varrho},$$

$$c(r) = \frac{2a_3}{r} \sinh\left(r\sqrt{\frac{\lambda}{D_A + D_B}}\right), \qquad \text{for } r \leq \bar{\varrho}.$$

To determine the constants a_2 and a_3, we use the continuity of c and its derivative at $r = \overline{\varrho}$. We obtain

$$a_2 = c_\infty \left\{ \sqrt{(D_A + D_B)/\lambda} \, \tanh\left(\overline{\varrho}\sqrt{\lambda/(D_A + D_B)}\right) - \overline{\varrho} \right\},$$

$$a_3 = c_\infty \sqrt{(D_A + D_B)/\lambda} \left(2\cosh\left(\overline{\varrho}\sqrt{\lambda/(D_A + D_B)}\right) \right)^{-1}.$$

The flux through the unit area of the boundary can be computed as

$$(D_A + D_B)\frac{\partial c}{\partial r}\bigg|_{r=\overline{\varrho}} = -\frac{(D_A + D_B)a_2}{\overline{\varrho}^2}.$$

The area of the sphere is $4\pi\overline{\varrho}^2$. Thus the total flux through the sphere boundary is $-4\pi(D_A + D_B)a_2$. Substituting for a_2, we get

$$4\pi(D_A + D_B)\left(\overline{\varrho} - \sqrt{(D_A + D_B)/\lambda}\,\tanh\left(\overline{\varrho}\sqrt{\lambda/(D_A + D_B)}\right)\right)c_\infty.$$

This quantity is equal to the rate constant of bimolecular reaction k_1 multiplied by the concentration of the chemical far from the reacting molecule c_∞. Dividing by c_∞, we derive (31). Let us note that we used diffusion to the ball to derive (31). This approximation can be justified using the more general evolution equation for the many particle distribution function [9].

Appendix F. Derivation of (34)–(36) and a numerical method for solving it

Let $c_i(r)$ be the concentration of molecules of A at distance r from the origin. Assuming that molecules of A only diffuse, their concentration at point r after the time interval Δt is given as

$$\int_0^\infty K(r, r'; \gamma)\, c_i(r')\, \mathrm{d}r' \tag{F.1}$$

where $K(r, r'; \gamma)$ is given by (35). Let us assume that the particles are removed, in the circle of radius $\overline{\varrho}$ and centered at origin, with probability P_λ, and then diffuse for time Δt. Then (F.1) is modified to

$$c_{i+1}(r) = (1 - P_\lambda)\int_0^1 K(r, r'; \gamma)\, c_i(r')\, \mathrm{d}r' + \int_1^\infty K(r, r'; \gamma)\, c_i(r')\, \mathrm{d}r'.$$

Equation (34) is an equation for the fixed point of this iterative scheme. The function $g(r)$ is the generalization of the radial distribution function (RDF) for bimolecular reaction at steady state [3] for arbitrary $P_\lambda \in [0, 1]$. Note that the RDF in [3] was only computed for $P_\lambda = 1$. The rate of removal of particles (at steady state) during one time step is given by the right hand side of (36). Comparing with κ, we obtain (36).

As discussed in Section 4.2, equations (34)–(36) are conditions relating the measurable parameters k_1, D_A and D_B with the parameters of the λ–$\overline{\varrho}$ model. Equations (34)–(36) have to be solved numerically before the stochastic simulation is executed. To solve (34), we will use the condition $g(r) \to 1$ as $r \to \infty$. Choosing S large, we can approximate $g(r) = 1$ for $r \geq S$. Let N_1 and N_2 be positive integers. We

consider the mesh $r_j = j/N_1$, for $j = 1, 2, \ldots, N_1$ and $r_j = 1 + (S-1)(j-N_1)/N_2$, for $j = N_1 + 1, \ldots, N_1 + N_2$. We discretize (34) as

$$g(r_i) = \frac{1 - P_\lambda}{N_1} \sum_{j=1}^{N_1} K(r_i, r_j; \gamma) g(r_j) + \frac{S-1}{N_2} \sum_{j=N_1+1}^{N_1+N_2} K(r_i, r_j; \gamma) g(r_j) + \int_S^\infty K(r_i, r'; \gamma) \, \mathrm{d}r'.$$

This is a linear system for $g(r_i)$, $i = 1, 2, \ldots, N_1 + N_2$, which can be solved, for example, by Gaussian elimination. Let us note that the right hand side of this system can be evaluated using the error function erf as

$$\int_S^\infty K(r_i, r'; \gamma) \, \mathrm{d}r' = \frac{\gamma^2 K(r_i, S; \gamma)}{S} + 1 - \frac{1}{2} \, \mathrm{erf} \left[\frac{S - r_i}{\gamma \sqrt{2}} \right] - \frac{1}{2} \, \mathrm{erf} \left[\frac{S + r_i}{\gamma \sqrt{2}} \right].$$

Substituting $g(r_i)$, $i = 1, 2, \ldots, N_1$, into (36), we compute κ. Repeating this computation for different values of γ and P_λ, we obtain the results presented in Figure 5. This graph or the corresponding look-up table can be used to implement the λ–$\overline{\varrho}$ model in a particle based simulator, as it has been done in [3] for the special case $P_\lambda = 1$.

References

[1] B. Alberts, A. Johnson, J. Lewis, M. Raff, K. Roberts, and P. Walter, *Molecular Biology of the Cell*, Garland Science, New York, 2002.

[2] S. Andrews, *Serial rebinding of ligands to clustered receptors as exemplified by bacterial chemotaxis*, Physical Biology **2** (2005), 111–122.

[3] S. Andrews and D. Bray, *Stochastic simulation of chemical reactions with spatial resolution and single molecule detail*, Physical Biology **1** (2004), 137–151.

[4] H. Berg, *Random Walks in Biology*, Princeton University Press, 1983.

[5] H. Berg and E. Purcell, *Physics of chemoreception*, Biophysical Journal **20** (1977), 193–219.

[6] S. Chandrasekhar, *Stochastic problems in physics and astronomy*, Reviews of Modern Physics **15** (1943), 2–89.

[7] R. DeVille, C. Muratov, and E. Vanden-Eijnden, *Non-meanfield deterministic limits in chemical reaction kinetics*, Journal of Chemical Physics **124** (2006), 231102.

[8] J. Dix and A. Verkman, *Crowding effects on diffusion in solutions and cells*, Annual Review of Biophysics **37** (2008), 247–263.

[9] M. Doi, *Stochastic theory of diffusion-controlled reaction*, Journal of Physics A: Mathematical and General **9** (1976), no. 9, 1479–1495.

[10] A. Einstein, *Über die von der molekularkinetischen Theorie der Wärme geforderte Bewegung von in ruhenden Flüssigkeiten suspendierten Teilchen*, Annalen der Physik **17** (1905), 549–560.

[11] S. Engblom, *Computing the moments of high dimensional solutions of the master equation*, Applied Mathematics and Computation **180** (2006), no. 2, 498–515.

[12] S. Engblom, L. Ferm, A. Hellander, and P. Lötstedt, *Simulation of stochastic reaction-diffusion processes on unstructured meshes*, Technical Report 2008-012, Dept of Information Technology, Uppsala University, Uppsala, Sweden, 2008.

[13] R. Erban and S. J. Chapman, *Reactive boundary conditions for stochastic simulations of reaction-diffusion processes*, Physical Biology **4** (2007), no. 1, 16–28.

[14] R. Erban, S. J. Chapman, K. Fisher, I. Kevrekidis, and L. Seymour, *Dynamics of polydisperse irreversible adsorption: a pharmacological example*, Mathematical Models and Methods in Applied Sciences (M3AS) **17** (2007), no. 5, 759–781.

[15] R. Erban, S. J. Chapman, I. Kevrekidis, and T. Vejchodsky, *Analysis of a stochastic chemical system close to a SNIPER bifurcation of its mean-field model*, SIAM Journal on Applied Mathematics **70** (2009), no. 3, 984–1016.

[16] R. Erban, S. J. Chapman, and P. Maini, *A practical guide to stochastic simulations of reaction-diffusion processes*, 35 pages, available as http://arxiv.org/abs/0704.1908, 2007.

[17] R. Erban and H. Othmer, *From individual to collective behaviour in bacterial chemotaxis*, SIAM Journal on Applied Mathematics **65** (2004), no. 2, 361–391.

[18] _____, *From signal transduction to spatial pattern formation in* E. coli*: A paradigm for multi-scale modeling in biology*, Multiscale Modeling and Simulation **3** (2005), no. 2, 362–394.

[19] _____, *Taxis equations for amoeboid cells*, Journal of Mathematical Biology **54** (2007), no. 6, 847–885.

[20] K. Fushimi and A. Verkman, *Low viscosity in the aqueous domain of cell cytoplasm measured by picosecond polarization microfluorimetry*, Journal of Cell Biology **112** (1991), no. 4, 719–725.

[21] D. Gillespie, *Exact stochastic simulation of coupled chemical reactions*, Journal of Physical Chemistry **81** (1977), no. 25, 2340–2361.

[22] _____, *Markov Processes, an introduction for physical scientists*, Academic Press, Inc., Harcourt Brace Jovanowich, 1992.

[23] _____, *The chemical Langevin equation*, Journal of Chemical Physics **113** (2000), no. 1, 297–306.

[24] J. Hattne, D. Fange, and J. Elf, *Stochastic reaction-diffusion simulation with MesoRD*, Bioinformatics **21** (2005), no. 12, 2923–2924.

[25] D.J. Higham, *An algorithmic introduction to numerical simulation of stochastic differential equations*, SIAM Review **43** (2001), no. 3, 525–546.

[26] S. Isaacson, *The reaction-diffusion master equation as an asymptotic approximation of diffusion to a small target*, SIAM Journal on Applied Mathematics **70** (2009), no. 1, 77–111.

[27] S. Isaacson and C. Peskin, *Incorporating diffusion in complex geometries into stochastic chemical kinetics simulations*, SIAM Journal on Scientific Computing **28** (2006), no. 1, 47–74.

[28] A. McKane and T. Newman, *Stochastic models in population biology and their deterministic analogs*, Physical Review E **70** (2004), 041902.

[29] J. Murray, *Mathematical Biology*, Springer Verlag, 2002.

[30] S. Northrup and H. Erickson, *Kinetics of protein-protein association explained by Brownian dynamics computer simulation*, PNAS **89** (1992), 3338–3342.

[31] J. Paulsson, O. Berg, and M. Ehrenberg, *Stochastic focusing: Fluctuation-enhanced sensitivity of intracellular regulation*, PNAS **97** (2000), no. 13, 7148–7153.

[32] A. Singer, Z. Schuss, A. Osipov, and D. Holcman, *Partially reflected diffusion*, SIAM Journal on Applied Mathematics **68** (2008), no. 3, 844–868.

[33] M. Smoluchowski, *Versuch einer mathematischen Theorie der Koagulationskinetik kolloider Lösungen*, Zeitschrift für physikalische Chemie **92** (1917), 129–168.

[34] J. Stiles and T. Bartol, *Monte Carlo methods for simulating realistic synaptic microphysiology using MCell*, Computational Neuroscience: Realistic Modeling for Experimentalists (E. Schutter, ed.), CRC Press, 2001, pp. 87–127.

[35] J. Thomas, *Numerical partial differential equations*, vol. 22, Springer Verlag, 1995.

[36] A. Tournier, P. Fitzjohn, and P. Bates, *Probability-based model of protein-protein interactions on biological timescales*, Algorithms for Molecular Biology **1** (2006), no. 25, 1–11.

[37] A. Twomey, *On the stochastic modelling of reaction-diffusion processes*, M.Sc. Thesis, University of Oxford, United Kingdom, September 2007.

[38] N. van Kampen, *Stochastic Processes in Physics and Chemistry*, 3rd ed., North-Holland, Amsterdam, 2007.

[39] J. van Zon and P. ten Wolde, *Green's-function reaction dynamics: a particle-based approach for simulating biochemical networks in time and space*, Journal of Chemical Physics **123** (2005), 234910.

[40] E. Zauderer, *Partial Differential Equations of Applied Mathematics*, John Wiley & Sons, 1983.